Standard Title Page - Report on Federally Funded Project

1. Report No. FHWA/VTRC 06-CR1	2. Government Accession No.	3. Recipient's Catalog No.
4. Title and Subtitle Fatigue Life Characterization of Superpave Mixtures at the Virginia Smart Road		5. Report Date August 2005 6. Performing Organization Code
7. Author(s) Imad L. Al-Qadi, Stacey Diefenderfer, and Amara Loulizi		8. Performing Organization Report No. VTRC 06-CR1
9. Performing Organization and Address Virginia Tech Transportation Institute 3500 Transportation Research Plaza Blacksburg, VA 24061		10. Work Unit No. (TRAIS) 11. Contract or Grant No. 53879
12. Sponsoring Agencies' Name and Address Virginia Department of Transportation 1401 E. Broad Street Richmond, VA 23219 FHWA P.O. Box 10249 Richmond, VA 23240		13. Type of Report and Period Covered Final 14. Sponsoring Agency Code
15. Supplementary Notes		

16. Abstract

Laboratory fatigue testing was performed on six Superpave HMA mixtures in use at the Virginia Smart Road. Evaluation of the applied strain and resulting fatigue life was performed to fit regressions to predict the fatigue performance of each mixture. Differences in fatigue performance due to field and laboratory production and compaction methods were investigated. Also, in-situ mixtures were compared to mixtures produced accurately from the job mix formula to determine if changes occurring between the laboratory and batch plant significantly affected fatigue life. Results from the fatigue evaluation allowed verification of several hypotheses related to mixture production and compaction and fatigue performance.

It was determined that location within the pavement surface, such as inner or outer wheelpath or center-of-lane, did not significantly affect laboratory fatigue test results, although the location will have significant effects on in-situ fatigue life. Also the orientation of samples cut from an in-situ pavement (parallel or perpendicular to the direction of traffic) had only a minor effect on the laboratory fatigue life, because the variability inherent in the pavement due to material variability is greater than the variability induced by compaction. Fatigue life of laboratory-compacted samples was found to be greater than fatigue life of field-compacted samples; additionally, the variability of the laboratory compacted mixture was found to be less than that of the field-compacted samples. However, it was also found that batch-plant production significantly reduces specimen variability as compared to small-batch laboratory production when the same laboratory compaction is used on both specimen sets. Finally, for Smart Road mixtures produced according to the job mix formula, the use of polymer-modified binder or stone matrix asphalt was shown to increase the expected fatigue life. However, results for all mixes indicated that fatigue resistance rankings might change depending on the applied strain level.

This study contributes to the understanding of the factors involved in fatigue performance of asphalt mixtures. Considering that approximately 95% of Virginia's interstate and primary roadways incorporate asphalt surface mixtures, and that fatigue is a leading cause of deterioration, gains in the understanding of fatigue processes and prevention have great potential payoff by improving both the mixture and pavement design practices.

17 Key Words	18. Distribution Statement
Fatigue life characterization, vibratory compaction, third point bending fatigue, pavement performance	No restrictions. This document is available to the public through NTIS, Springfield, VA 22161.

19. Security Classif. (of this report)	20. Security Classif. (of this page)	21. No. of Pages	22. Price
Unclassified	Unclassified	60	

Form DOT F 1700.7 (8-72) Reproduction of completed page authorized

FINAL CONTRACT REPORT

FATIGUE LIFE CHARACTERIZATION OF SUPERPAVE MIXTURES AT THE VIRGINIA SMART ROAD

I. L. Al-Qadi, Ph.D., P.E.
Professor, Department of Civil and Environmental Engineering
Director, Advanced Transportation Research and Engineering Laboratory
University of Illinois at Urbana Champaign

S. Reubush Diefenderfer
Research Scientist
Virginia Transportation Research Council

A. Loulizi, Ph.D.
Research Associate
Virginia Tech Transportation Institute

Project Managers
Thomas E. Freeman, P.E., Virginia Transportation Research Council
Stacey Reubush Diefenderfer, Virginia Transportation Research Council

Contract Research Sponsored by
Virginia Transportation Research Council

Virginia Transportation Research Council
(A Cooperative Organization Sponsored Jointly by the
Virginia Department of Transportation and
the University of Virginia)

Charlottesville, Virginia

August 2005
VTRC 06-CR1

NOTICE

The project that is the subject of this report was done under contract for the Virginia Department of Transportation, Virginia Transportation Research Council. The contents of this report reflect the views of the authors, who are responsible for the facts and the accuracy of the data presented herein. The contents do not necessarily reflect the official views or policies of the Virginia Department of Transportation, the Commonwealth Transportation Board, or the Federal Highway Administration. This report does not constitute a standard, specification, or regulation.

Each contract report is peer reviewed and accepted for publication by Research Council staff with expertise in related technical areas. Final editing and proofreading of the report are performed by the contractor.

ABSTRACT

Laboratory fatigue testing was performed on six Superpave HMA mixtures in use at the Virginia Smart Road. Evaluation of the applied strain and resulting fatigue life was performed to fit regressions to predict the fatigue performance of each mixture. Differences in fatigue performance due to field and laboratory production and compaction methods were investigated. Also, in-situ mixtures were compared to mixtures produced accurately from the job mix formula to determine if changes occurring between the laboratory and batch plant significantly affected fatigue life. Results from the fatigue evaluation allowed verification of several hypotheses related to mixture production and compaction and fatigue performance.

It was determined that location within the pavement surface, such as inner or outer wheelpath or center-of-lane, did not significantly affect laboratory fatigue test results, although the location will have significant effects on in-situ fatigue life. Also the orientation of samples cut from an in-situ pavement (parallel or perpendicular to the direction of traffic) had only a minor effect on the laboratory fatigue life, because the variability inherent in the pavement due to material variability is greater than the variability induced by compaction. Fatigue life of laboratory-compacted samples was found to be greater than fatigue life of field-compacted samples; additionally, the variability of the laboratory compacted mixture was found to be less than that of the field-compacted samples. However, it was also found that batch-plant production significantly reduces specimen variability as compared to small-batch laboratory production when the same laboratory compaction is used on both specimen sets. Finally, for Smart Road mixtures produced according to the job mix formula, the use of polymer-modified binder or stone matrix asphalt was shown to increase the expected fatigue life. However, results for all mixes indicated that fatigue resistance rankings may change depending on the applied strain level.

This study contributes to the understanding of the factors involved in fatigue performance of asphalt mixtures. Considering that approximately 95% of Virginia's interstate and primary roadways incorporate asphalt surface mixtures, and that fatigue is a leading cause of deterioration, gains in the understanding of fatigue processes and prevention have great potential payoff by improving both the mixture and pavement design practices.

INTRODUCTION

Selection of appropriate highway materials with respect to climatic and loading conditions can significantly contribute to an increase in expected pavement service life and can lead to notable long-term savings. With these considerations, the Superpave (Superior Performing Asphalt Pavements) mixture design protocol was developed as a product of the Strategic Highway Research Program (SHRP), a five-year, $150 million program designed to improve the performance and durability of US roads and highways (Asphalt Institute, 1996). The system is intended to incorporate performance-based materials characterization with designs for environmental and traffic conditions to improve highway performance.

Utilizing an understanding of the interaction between climate, traffic, and pavement performance, Superpave mixtures are developed to perform under site-specific traffic and climatic loading conditions. They are designed to resist, in particular, deterioration due to low temperature cracking, fatigue, and permanent deformation. Low temperature cracking is caused by excessive tensile stresses induced over time by thermal gradients within pavements. Permanent deformation, commonly called rutting, is generally attributed to insufficiently designed pavements or poor subgrades and is characterized as a permanent change in the form of a pavement or pavement layer (Roberts *et al*., 1996). Fatigue is the process by which the pavement deteriorates through cracking because of small built-up irrecoverable strains induced by repeated loading over time (Khalid, 2000a, 2000b).

The potential for these distresses is usually evaluated through laboratory testing performed on laboratory-produced specimens. However, production of laboratory specimens differs significantly from production of hot mix asphalt (HMA) for roadways. Also, differences have been shown to exist for test results between specimens produced in the laboratory using different compaction methods and road cores (Button *et al*., 1994; Consuegra *et al*., 1989; Harvey and Monismith, 1993; Khan *et al*., 1998; Masad *et al*., 1999). The method of compaction to be utilized in producing fatigue specimens, vibratory compaction, is relatively new and its performance in replicating field specimens has not yet been substantiated. Evaluation of compaction effects between the laboratory and field can give valuable insight into adjusting design procedures such that in situ material will more accurately reflect design performance. Six different Superpave mixtures are in service at the Virginia Smart Road, offering the opportunity to evaluate these effects on HMA mixtures through in-service testing and laboratory characterization.

Fatigue in HMA Pavements

Damage to asphalt pavements caused by repetitive stresses and strains due to climatic and traffic-applied loading is considered fatigue, and is one of the primary distress mechanisms in asphalt pavements. Fatigue is the process by which the pavement deteriorates through cracking because of small built-up irrecoverable strains induced by repeated loading over time (Khalid, 2000a, 2000b). These strains accumulate because of the viscoelastic properties of HMA. When loads are removed, induced strains are not completely recovered and these accumulate over time. Fatigue cracking is generally thought to begin at the bottom of the HMA layer, as this area is

placed in a state of tensile strain from the stresses caused by repeated traffic loading. Fatigue is a two-stage process consisting of microcrack growth and healing and macrocrack growth and healing. Both of these processes are thought to be governed by Paris' law (Little *et al*., 2001). After crack initiation at the bottom of the asphalt layer, cracks propagate upward, and may eventually result in a network of cracks in the asphalt surface, which gives fatigue cracking its more common name, alligator cracking. Although less commonly accepted, fatigue may also initiate at the top surface of the pavement. This is hypothesized to be due to non-uniform three-dimensional contact traction and pressure distribution between the pavement and vehicle tire (Collop and Cebon, 1995). Fatigue cracking also may be initiated at both the top and bottom of asphalt layers due to horizontal tensile strains induced by daily temperature cycles (Collop and Cebon, 1995).

Other aspects of HMA behavior that must be accounted for in the analysis of fatigue include temperature and loading effects. As a viscoelastic material, asphalt mixtures are temperature sensitive in their response to applied loads. At high temperatures, HMA behaves as a viscous liquid; at low temperatures, it behaves as an elastic solid. Because of this, loads have greater effect at high temperatures. Additionally, the duration of the loading affects response. Since fatigue is caused by an accumulation of strains, the ability of asphalt mixtures to "relax" or recover strains upon unloading complicates the task of evaluating fatigue. Over time, the residual stress in pavements will relax since there are generally sufficient rest periods between applications of traffic loads. Fatigue specimens in the laboratory will also undergo this effect; however, as there are not sufficient relaxation periods between load applications for total recovery, the residual stresses will accumulate.

It is well documented in the literature that laboratory fatigue responses are considerably more conservative than the actual response seen in pavements. This has been postulated to be due to differences in crack propagation, healing effects due to rest periods, use of simple loading patterns, temperature effects, and influences of surface cracking. The effects of temperature and rest periods have been addressed in fatigue evaluation previously by the introduction of shift factors (Balbissi, 1983; Tseng and Lytton, 1990); however, the accuracy of such factors depends on the availability of field data for calibration and verification. Additional differences between laboratory and in-situ fatigue life are due to the use of different fatigue design criteria amongst researchers. Shift factors have been introduced to attempt to relate laboratory results with expectations for in-situ pavements. Many of these factors are simply general factors applied to the expected life and based on phenomenological fatigue studies, rather than mechanistic evaluation. These factors are reported by a number of researchers and range in value from approximately 0.95 to 20 (Majidzadeh *et al*., 1973; Monismith, 1981; Van Dijk, 1975), depending on the method of laboratory testing and the make-up of the applicable pavement.

Many researchers have identified material properties that have significant effects on fatigue life. Harvey and Monismith (1993) evaluated the effects of binder type, aggregate type, fines content, air void content, compaction method, mixing viscosity, and compaction viscosity on the fatigue life of mixtures using the third point loading flexural beam test. It was found that mixture stiffness was sensitive to binder type, air void content, mixing viscosity, and compaction method. The fatigue life was found to be sensitive to binder type, fines content, air void content,

mixing and compaction viscosities, and compaction method. SHRP Project A-003 (SHRP, 1994) included the development of a standardized testing method for laboratory evaluation of fatigue. The resulting test method utilized the third point loading flexural beam fatigue test. During the test method development, experimentation was performed to evaluate the effects of asphalt content and air void content on the fatigue life of a single asphalt-aggregate mixture. It was found that the asphalt content and air void content had significant effects on initial flexural stiffness, fatigue life, and cumulative dissipated energy. Increasing the asphalt content resulted in decreased mixture stiffness, and increases in fatigue life and cumulative dissipated energy. Increasing the air voids resulted in decreases in mixture stiffness, fatigue life, and cumulative dissipated energy. Deacon *et al*. (1995a) evaluated fatigue properties using the third point loading flexural beam fatigue test and concluded that aggregate structure, as induced by mixture compaction, has a significant effect on mixture fatigue properties. Harvey and Tsai (1996) evaluated fatigue performance of several mixtures and determined that lower air voids are of clear benefit to fatigue life and initial stiffness. The study also found that increased asphalt content increased fatigue life and reduced mixture stiffness. The effects of mixture segregation on fatigue life were evaluated by Khedaywi and White (1996) and it was found that fatigue life significantly decreased with increasing segregation.

PURPOSE AND SCOPE

Pavement fatigue response to loading, which is defined by the number of applied loads and strains, can be predicted from empirical equations. However, the empirical methods suffer from several shortcomings, including the lack of calibration for current Superpave mixture properties and differences in testing methodology. Additionally, assumptions related to material properties are made in using these equations that render them less accurate than desired.

This report presents findings for the evaluation of fatigue performance of six Superpave surface mixtures with the intent of identifying mixtures that may be more prone to fatigue occurrence. These findings are necessary for effective flexible pavement analysis and design. It should be understood that these experimental results are only applicable to the mixtures tested; due to the small sample size, general conclusions cannot be drawn.

METHODS

The flexible pavement portion of the Virginia Smart Road consists of 12 sections having different designs, as shown in Table 1. All designations are in accordance with the Virginia Department of Transportation (VDOT) specifications (VDOT, 1997 and 1999). Seven different wearing surface mixes were used: five different Superpave mixtures, an open-graded friction course (OGFC), and a stone matrix asphalt (SMA). An asphalt base mix with a maximum nominal aggregate size of 25 mm (BM-25.0) was used in all the sections with different thicknesses varying from 100 to 225 mm. An open graded drainage layer (OGDL) was incorporated in nine sections with a thickness of 75 mm. This drainage layer was stabilized with

Table 1. Smart Road flexible pavement designs.

Section	Wearing Surface 38mm	BM-25.0 (mm)	SM-9.5A (mm)	OGDL (mm)	CTA (mm)	Aggregate (mm)
A	SM-12.5D	150	-	75	150	175
B	SM-9.5D	150	-	75	150	175/ GT
C	SM-9.5E	150	-	75	150	175/ GT
D	SM-9.5A	150	-	75	150	175/ GT
E	SM-9.5D	225	-	-	150	75/ GT
F	SM-9.5D	150	-	-	150	150
G	SM-9.5D	100	50	-	150	150/ GT
H	SM-9.5D	100	50	75	150	75
I	SM-9.5A*	100/RM	50	75	150	75
J	SM-9.5D	225	-	75/MB	-	150
K	OGFC+SM-9.5D	225/SR	-	75	-	150
L	SMA-12.5	150/RM	-	75	150	75

* High laboratory compaction

SR: Stress Relief Geosynthetic; GT: Woven Geotextile/Separator; RM: Reinforcing Mesh; MB: Moisture Barrier

asphalt in seven sections and with cement in two sections (K and L). A cement treated aggregate (CTA) base was used at a thickness of 150 mm in ten sections. An aggregate subbase layer was placed above the subgrade in all sections with thicknesses varying from 75 to 175 mm. Different types of geosynthetics and reinforcing meshes were also incorporated in some sections.

An experimental testing program was performed at the Virginia Smart Road with an overall purpose of characterizing and comparing the fatigue performance of the five Superpave surface mixtures and the SMA mixture. Base mixtures were not tested at this time due to limitations in specimen production. Several different methods of mixture preparation were utilized: field-mixed and field-compacted (F/F); field-mixed and laboratory-compacted (F/L); laboratory-mixed and laboratory-compacted (L/L); and laboratory-mixed according to job mix formula and laboratory-compacted (D/L). The F/F samples were cut from the pavement in section C during August of 2001. The F/L samples were obtained during construction as loose samples randomly taken from either incoming trucks or the paver. These samples were then reheated and compacted in the laboratory. L/L samples were produced to match the gradation and asphalt content found from the F/L samples, since discrepancies were found between the F/L gradations and asphalt content and the job mix formula; thus, the D/L samples were prepared and compacted in the laboratory to meet the requirements of the design specifications. A summary of fatigue testing specimens is presented in Table 2.

Laboratory compaction was performed using a PTI asphalt vibratory compactor as shown in Figure 1. Specimens were compacted to the average voids in total mix (VTM) measured from cored F/F specimens. This was performed by determining the mix volume, and thus mass, necessary to provide the correct air void content after compaction to a specific specimen height. This method was utilized as there are no specifications for compaction in the vibratory compactor. These values are presented in Table 3. All specimens were measured and weighed

Table 2. Summary of fatigue testing specimens.

Mixture	Section	Field / Field	Field / Lab	Lab / Lab	Design / Lab
SM-12.5D	A		10	10	10
SM-9.5D	B		10	10	10
SM-9.5E	C	36	10	10	48
SM-9.5A	D		10	10	10
SM-9.5D	E		10	10	
SM-9.5D	F		10		
SM-9.5D	G		10		
SM-9.5D	H		10		
SM-9.5A*	I		10	10	10
SM-9.5D	J		10	10	
SM-12.5A	L		10	10	10

* High laboratory compaction

Figure 1. PTI Vibratory compactor.

after compaction to determine volumetric properties. Laboratory-compacted specimens were approximately 50.8 mm x 63.5 mm x 381 mm rectangular beams. F/F specimens cut from the in-situ pavement were approximately 35 to 45 mm in thickness, rather than the preferred 50.8 mm, due to the thickness of the wearing surface at the Virginia Smart Road. Specimens were stored at 25ºC until testing was performed.

Table 3. Target Voids in Total Mix (VTM) for Vibratory Compaction.

Mixture	Section	Field / Lab	Lab / Lab	Design / Lab
SM-12.5D	A	3.2	5.2	4.8
SM-9.5D	B	3.6	1.8	5.0
SM-9.5E	C	2.3	2.0	1.3
SM-9.5A	D	1.3	0.9	3.6
SM-9.5D	E	1.4	1.9	
SM-9.5D	F	3.6		
SM-9.5D	G	3.6		
SM-9.5D	H	4.1		
SM-9.5A*	I	1.5	6.0	4.3
SM-9.5D	J	7.5	4.6	
SMA-12.5	L	1.8	1.8	2.3

* High laboratory compaction.

Third Point Beam Fatigue Test

Characterization of fatigue life has been a well-recognized concern in pavement design for many years, since at least 1948 (Hveem and Carmany, 1948). Laboratory evaluation of fatigue generally focuses on direct applications of loads. There are several common methods of fatigue testing, including simple flexure, supported flexure, direct axial, and diametral (Matthews *et al*., 1993). Simple flexure tests are the most common and include methods whereby loads are applied repeatedly or sinusoidally to rectangular beams with center point (Khalid, 2000a) or third-point loading (Deacon *et al*., 1994, 1995a, 1995b; Harvey and Monismith, 1993; Harvey *et al*., 1994; Harvey and Tsai, 1996; Khalid, 2000b; Khedaywi and White, 1996; Maupin, 1972, 1977; Radziszewski, 1997; Read and Brown, 1996; Read and Collop, 1997; Sousa *et al*., 1998; Tayebali *et al*., 1992, 1994, 1996a, 1996b). Loads may also be applied sinusoidally to rotating cantilever beams (Pell and Cooper; 1975) or sinusoidally to trapezoidal beams (Francken and Verstraeten, 1974), although these modes are less common than the methods employing rectangular beams. Supported flexure tests apply loading to a beam supported on an elastic base; this better reflects actual field conditions but requires special equipment so is less generally performed (Matthews *et al*., 1993; Ramsamooj, 1980, 1991). Direct axial tests are performed by applying loads in the axial direction (Brennan *et al*., 1996; Von Quintus *et al*., 1982). Diametral testing is performed in the indirect tensile mode by applying a haversine loading pulse. This method of fatigue testing is commonly used (Adedimila and Kennedy, 1976; Baladi *et al*., 1988; Bell *et al*., 1984; Khalid, 2000b; Kim *et al*., 1992; Leahy *et al*., 1995; Von Quintus *et al*., 1982) and is considered an effective means of characterizing fundamental material properties.

Fatigue testing may be performed under two loading conditions: controlled-stress or controlled-strain. These are important as fatigue characteristics are generally expressed as relationships between the initial stress or strain and the number of load repetitions to failure. The determination of controlled-stress or –strain is important as it relates to the in-situ pavement structure. Controlled stress testing is associated with evaluation of thick asphalt layers (greater

than approximately 150 mm) except when the asphalt is extremely weak or the support exceedingly stiff, and controlled strain testing is associated with thin asphalt layers (less than approximately 50 mm) unless the asphalt is extremely stiff or the support very weak (Monismith and Deacon, 1969). Additionally, it has been reported that fatigue lives under controlled-strain conditions are approximately 2.4 times greater than those under controlled-stress conditions (Tayebali *et al*., 1994). However, it has also been found that the ranking of mixtures, in terms of fatigue performance, is not affected by the mode of loading (SHRP, 1994). This determination from fatigue testing through the SHRP A-003 program has resulted in specifications for a third-point bending fatigue test in the controlled-strain mode (Deacon *et al*., 1995a, 1995b; Matthews and Monismith, 1993; Matthews *et al*., 1993; SHRP, 1994; Tayebali *et al*., 1992, 1996a,b).

Fatigue life testing for this study was performed using the third-point mode of loading flexural test under controlled-strain conditions, as specified in the AASHTO TP8-94 and SHRP M-009 protocols. This method of test was chosen due to its ease of use and understanding, as well as its adoption by SHRP as a standard. The controlled-strain condition was chosen for use as all HMA mixtures to be tested are surface course mixtures and are present at the Virginia Smart Road as a thin pavement layer, approximately 38 to 76 mm in thickness.

The third point beam fatigue test applies loading at points located at one-third distances from the beam ends, as shown in Figure 2. This produces uniform bending in the central third of the specimen and significantly simplifies analysis. The test is run until failure occurs; however, there is dispute concerning the definition of failure for the controlled strain test, as it is very difficult to reach a physical failure via fracture. Currently, specifications (AASHTO TP8-94 and SHRP M-009) set the criterion for failure as occurring when there is a 50% reduction in the measured stiffness; initial stiffness is measured after 50 applied load cycles. Several researchers (Ghuzlan and Carpenter, 2000; Kim *et al*., 1997) have introduced alternative methods to this, each of which have been proposed to avoid the issues of mode-of-loading, temperature, loading frequency, and rest periods, which have been shown to influence fatigue life. However, none of these methods has been fully validated, nor proven to be uninfluenced by the aforementioned

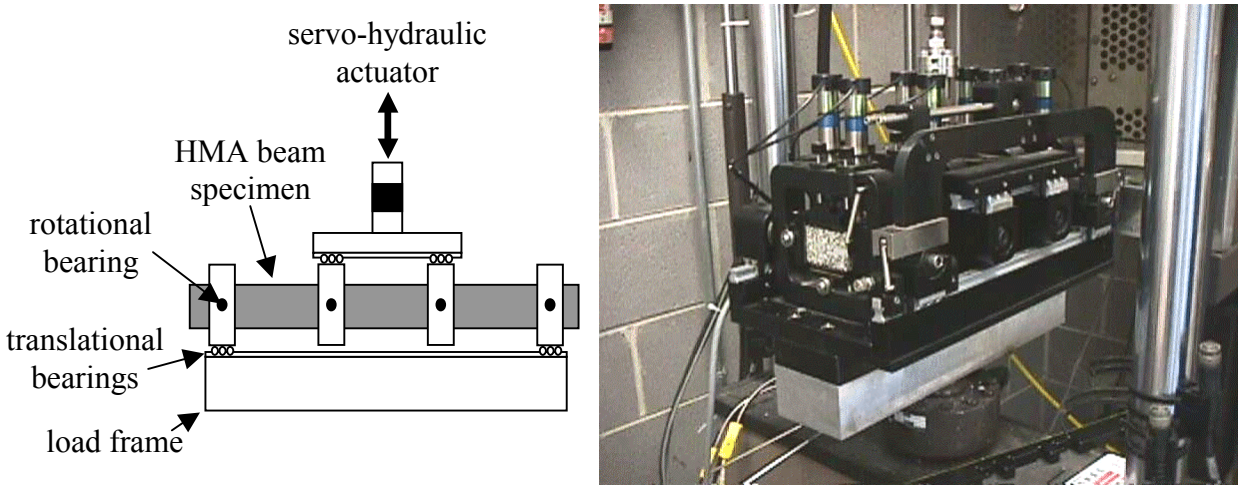

Figure 2. Third point loading beam fatigue test apparatus.

issues. For this research, the 50% reduction of initial stiffness was utilized as failure criterion in accordance with specifications AASHTO TP8-94 and SHRP M-009. This method of failure definition was chosen to comply with specifications as well as to provide a standard method of test comparable to that performed by other researchers, in the assumption that future comparisons may be made.

Measurement and Quantification of Fatigue Response in Third Point Bending

Fatigue testing was performed at a temperature of 25ºC. The strain levels for the replicate sets of four specimens each were chosen to be between 200 and 800 microstrain such that the specimen life ranged from approximately 5000 to 350000 cycles, with the failure criterion being 50% reduction of the initial stiffness. Testing was performed in the controlled-strain mode of loading at a frequency of 10 Hz. Raw data collected from the testing included beam deflection, applied load, and phase angle. Deflections were measured using a LVDT located within the servo-hydraulic actuator employed to apply the deflection. The resulting forces were measured through the fatigue fixture using a load cell mounted beneath the fixture. Data analysis software provided by the servohydraulic equipment manufacturer was used to calculate strain, stress, phase angle, mixture stiffness, dissipated energy per cycle, and cumulative dissipated energy according to the methodology specified in AASHTO TP8-94 and SHRP M-009. The maximum tensile stress is computed as:

$$\sigma_t = \frac{3\,a\,P}{w\,h^2} \tag{1}$$

where

σ_t = maximum tensile stress, kN/mm^2,
L = beam span, mm,
a = L / 3, mm,
P = measured load, kN,
w = beam width, mm, and
h = beam height, mm.

Maximum tensile strain is determined as:

$$\varepsilon_t = \frac{12\,h\,\delta}{3L^2 - 4a^2} \tag{2}$$

where

ε_t = maximum tensile strain, mm/mm, and
δ = beam deflection at central span, mm.

Stiffness is calculated as follows:

$$S = \frac{\sigma_t}{\varepsilon_t} \tag{3}$$

where S is the beam stiffness in Pa.

The phase angle is expressed as:

$$\phi = 360 \cdot f \cdot s \tag{4}$$

where

ϕ = phase angle, degrees,
f = load frequency, Hz, and
s = time lag between P_{max} and δ_{max}, sec.

Fatigue damage is related to the amount of energy dissipated in the specimen during testing. This is considered appropriate for asphalt mixtures, as the dissipated energy can be used to explain the decrease in mechanical properties, such as flexural stiffness, during testing. The dissipated energy per unit volume per cycle is determined as:

$$w_i = \pi \sigma_i \varepsilon_i \sin \phi_i \tag{5}$$

where

w_i = dissipated energy at load cycle i, kN-mm/mm^3,
σ_i = stress amplitude at load cycle i, kN/mm^2,
ε_i = strain amplitude at load cycle i, mm/mm, and
ϕ_i = phase angle between stress and strain wave signals, degrees.

The total, or cumulative dissipated energy can then be determined:

$$W_{fat} = \sum_{i=1}^{n} w_i \tag{6}$$

where W_{fat} is the cumulative dissipated energy at failure. The cumulative dissipated energy may be related to fatigue life as follows (Van Dijk, 1975):

$$W_{fat} = A \cdot (N_f)^z \tag{7}$$

where

N_f = number of cycles to failure, and
A and z = experimentally determined coefficients.

This relationship has been found to be dependent on the mixture formulation (Tayebali *et al*., 1992; Van Dijk, 1975; Van Dijk and Visser, 1977). Dissipated energy can be applied to the prediction of crack initiation. Pronk (1997) found that if the ratio of dissipated energy up to a number of cycles, N, to dissipated energy at that N is plotted versus N, microcrack initiation can be determined as the point where a sharp change in the slope of the line is observed.

Results of fatigue testing are generally interpreted in terms of a relationship between applied stress or strain and fatigue life. For the strain approach, this results in a relationship of the following form, commonly known as the Wöhler relationship:

$$N_f = K\left(\frac{1}{\varepsilon_0}\right)^n \tag{8}$$

where

N_f = fatigue life,
K and n = mix-dependent constants (Matthews and Monismith, 1993; Irwin and Gallaway, 1974; van Dijk and Visser, 1977), and
ε_0 = applied strain amplitude.

An additional parameter can be introduced into the general fatigue life equation to account for variations in loading and frequency:

$$N_f = K_1 \left(\frac{1}{\varepsilon}\right)^{K_2} \left(\frac{1}{S_0}\right)^{K_3} \quad (9)$$

where S_0 is the mixture initial stiffness and K_1, K_2, and K_3 are regression constants. However, Harvey and Tsai (1996) offer experimental results that indicate that stiffness should not be included in models used for evaluation of fatigue life, as conflicting results were found as to the effect of stiffness on fatigue life. For this study, there were too few experimental values to determine the necessity of including stiffness in the fatigue life prediction equation.

RESULTS AND DISCUSSION

As previously discussed, data collected during fatigue testing was used to determine the applied tensile strain and resulting stress, mixture stiffness, phase angle between stress and strain, dissipated energy per cycle, and cumulative dissipated energy for each specimen tested. These results were used to determine fatigue curves characteristics for each tested mixture, compare mixture performance and characteristics, and compare effects of differing production and compaction methods.

Linear regression was performed on $\log_e$-transformed data to determine the values of K and N in equation 8. These values are presented in Table 4 and an example plot of the relationship for the F/L SM-12.5D sample is shown in Figure 3. Similar plots for each tested HMA are available by request. Linear regression was also utilized with the $\log_e$-transformed data to determine the values of K_1, K_2, and K_3 for equation 9; however, these results indicated that the stiffness was unnecessary to fatigue life characterization, as the introduction of the stiffness variable caused instability in the regression and resulted errors for the determination of all coefficients. Thus, it was determined that equation 8 is sufficient for fatigue life characterization as performed in this study.

Evaluation of Location and Orientation of Fatigue Samples

Slabs having dimensions of approximately 0.6 m x 0.6 m were saw-cut from the in-situ pavement during August of 2001 for fatigue testing. These samples were taken from locations in the inner and outer wheelpaths and in the center of the lane. Fatigue specimens were cut from the slabs having two orientations: parallel to traffic (from inner wheelpath location) and perpendicular to traffic (from center of lane, inner and outer wheelpath locations). These samples were tested to determine if specimen location or orientation is significant in laboratory fatigue testing.

A plot of the fatigue results is shown in Figure 4; the samples noted as “CL-PP,” “OWP-PP,” and “IWP-PP” were cut with the beam length perpendicular to the direction of traffic and were located in the center of the lane, outer wheelpath, and inner wheelpath, respectively; samples noted as “IWP-PL” were cut from the inner wheelpath with the beam length being

Table 4. Coefficients K and n for equation 8.

Section	Mix	K	n	R^2
Field-produced, Field-compacted				
C - Center of lane*	SM-9.5E	4.0981×10^{-10}	-4.5846	0.83
C - Outer wheel path*		1.6281×10^{-8}	-4.0459	0.87
C - Inner wheel path*		1.8988×10^{-11}	-6.1547	0.94
C - Inner wheel path**		4.0751×10^{-13}	-5.4374	0.91
Field-produced, Laboratory-compacted				
I	SM-9.5A#	3.8912×10^{-15}	-5.5745	0.99
D	SM-9.5A	4.8443×10^{-10}	-4.1864	0.98
B	SM-9.5D	3.3150×10^{-9}	-3.8650	0.84
EFGH	SM-9.5D	7.6245×10^{-14}	-5.2199	0.95
J	SM-9.5D	1.2748×10^{-13}	-5.0413	0.96
C	SM-9.5E	9.9898×10^{-18}	-6.5922	0.93
A	SM-12.5D	2.7898×10^{-15}	-5.6455	0.95
L	SMA-12.5	5.7999×10^{-18}	-6.5740	0.87
Laboratory-produced, Laboratory-compacted				
I	SM-9.5A#	7.9466×10^{-13}	-4.8336	0.99
D	SM-9.5A	4.6498×10^{-12}	-4.6644	0.99
B	SM-9.5D	3.6421×10^{-14}	-5.2555	0.98
J	SM-9.5D	3.1378×10^{-15}	-5.5657	0.99
EFGH	SM-9.5D	1.2320×10^{-13}	-5.1814	0.98
C	SM-9.5E	1.4900×10^{-9}	-3.9916	0.91
A	SM-12.5D	1.0071×10^{-13}	-5.1962	0.98
Job Mix Formula, Laboratory-produced, Laboratory-compacted				
I	SM-9.5A#	2.0197×10^{-12}	-4.6670	0.95
D	SM-9.5A	5.3113×10^{-13}	-4.9437	0.98
B	SM-9.5D	2.8542×10^{-14}	-5.3580	0.95
C	SM-9.5E	1.6751×10^{-16}	-6.1179	0.94
A	SM-12.5D	4.2797×10^{-13}	-4.9849	0.98
L	SMA-12.5	6.1385×10^{-7}	-3.3251	0.69

* Beams cut with longest dimension perpendicular to traffic

** Beams cut with longest dimension parallel to traffic

High Laboratory Compaction

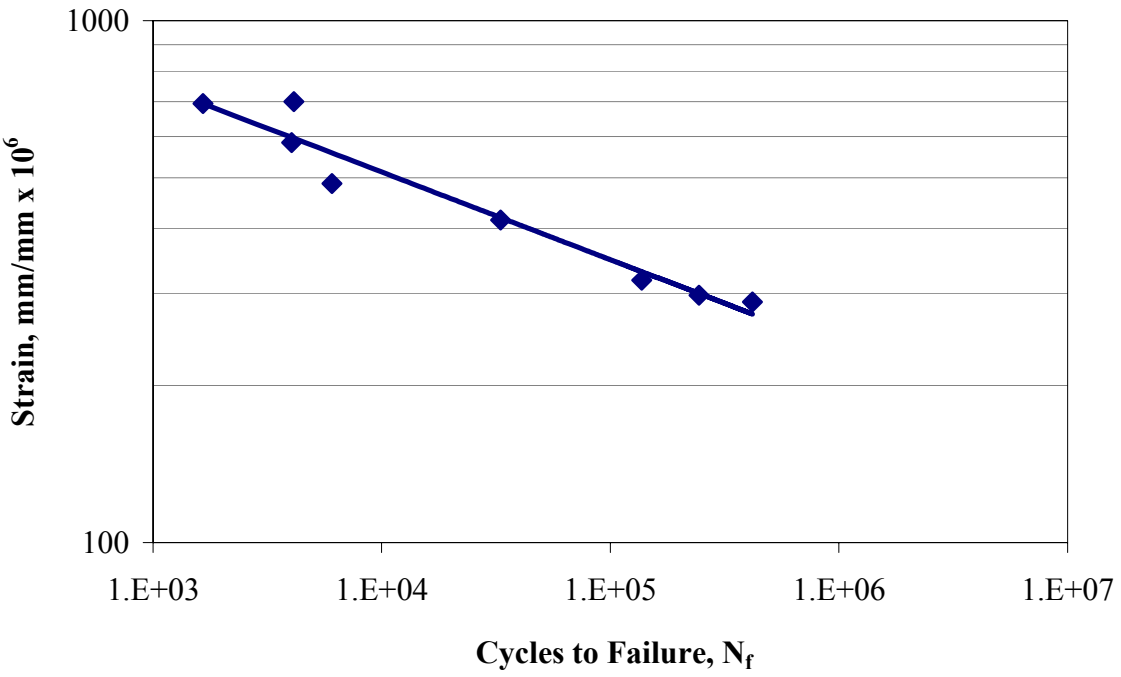

Figure 3. Example S-N plot for SM-12.5D, F/L, section A.

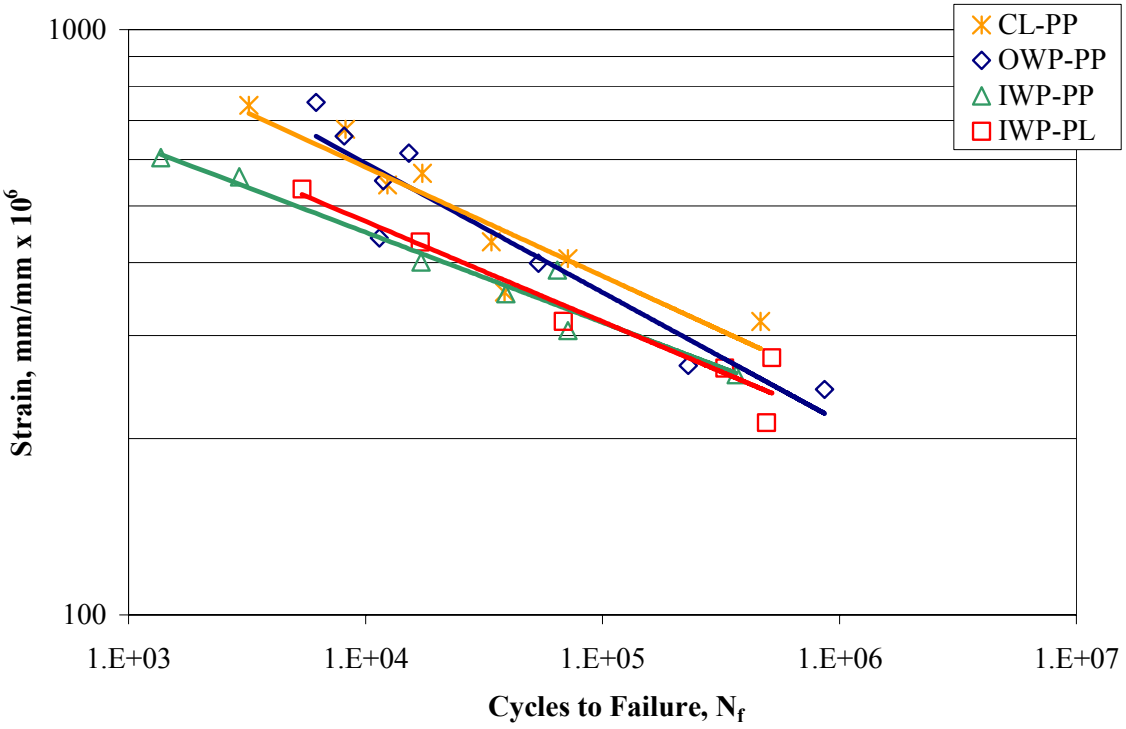

Figure 4. Comparison of location and direction of field samples.

parallel to traffic. Analysis of variance was performed to determine if significant differences exist between the samples located in the inner wheelpath and cut with opposing orientations to traffic. Results showed that no significant differences existed with respect to the orientation of the samples. This indicates that the direction of roller compaction may not have great significance in the determination of laboratory fatigue life.

Analysis to determine if location within the lane is a significant factor in fatigue life was inconclusive. Intuition notes that the fatigue life at the center of the lane should exceed that of the wheelpath in pavements, due to the wheel-loading pattern. However, in the laboratory, these differences are not present as each sample set is loaded in similar fashion; thus the evaluation of location serves more as an indication of compaction variability. There are visually significant differences shown in Figure 5 between the measured fatigue life for the inner wheelpath samples and for those located in the outer wheelpath and center of lane; however the differences were not found to be statistically significant, due to the variability in test results within each sample. Air void differences do not appear to explain this difference, as the average air voids for the inner wheelpath samples were found to be 12.9% and 6.8% for sample sets cut parallel and perpendicular to the direction of traffic, respectively, while the average air voids for sets located in the outer wheelpath and center of lane were 7.5% and 7.4%, respectively. This indicates that the variability seen across the lane width is less than the variability due to mixture and compaction effects within each small area (approximately 0.6 m x 0.6 m) from which the samples were cut.

Evaluation of Differences between Field and Laboratory Production and Compaction

Volumetric properties of fatigue specimens were determined from the dimensions and weights taken after compaction. Voids in total mix (VTM), voids in mineral aggregate (VMA), and voids filled with asphalt (VFA) were calculated from the specimen volumes, masses, and asphalt contents. Volumetric properties are presented in Tables 5 through 8. These figures indicate that considerable difference may exist between target void properties and those actually achieved using the vibratory compactor. These discrepancies likely are a function of the geometric configuration of the mold and compaction process; to reach very low percentages of voids, increased pressure must be exerted on the HMA mixture that may lead to aggregate fracturing during compaction. Comparison of volumetric results for the D/L samples reinforces the idea that the vibratory compactor has difficulties compacting to lower VTM targets. This

Table 5. Volumetric properties of F/F samples.

Section	Mix	Location	Asphalt (%)	VTM (%)	VMA (%)	VFA (%)
C-FF	SM-9.5E	CL-PP	5.8	7.5	19.4	61.7
		OWP-PP		7.4	19.3	62.8
		IWP-PP		12.8	24.0	47.2
		IWP-PL		6.8	18.8	64.1

Table 6. Volumetric properties of D/L samples.

Section	Mix	Asphalt (%)	VTM (%)		VMA (%)		VFA (%)	
			Gyratory	Vibratory	Gyratory	Vibratory	Gyratory	Vibratory
A-DL	SM-12.5D	5.6	4.8	8.9	16.8	20.4	71.4	56.5
B-DL	SM-9.5D	5.3	5.0	9.6	15.5	19.6	68.0	51.3
C-DL	SM-9.5E	6.2	1.3	8.0	14.9	20.6	91.4	61.6
D-DL	SM-9.5A	6.3	3.6	8.0	17.0	20.8	78.7	61.6
I-DL	SM-9.5A *	5.4	4.3	10.8	15.7	21.5	72.5	49.5
L-DL	SMA-12.5	6.3	2.3	10.5	15.9	23.0	85.3	54.5

* Designed using high laboratory compaction.

Table 7. Volumetric properties of F/L samples.

Section	Mix	Asphalt (%)	VTM (%)		VMA (%)		VFA (%)	
			Gyratory	Vibratory	Gyratory	Vibratory	Gyratory	Vibratory
A-FL	SM-12.5D	5.9	3.2	7.6	15.7	19.6	79.8	61.0
B-FL	SM-9.5D	4.7	3.6	9.0	12.5	17.4	71.6	48.6
C-FL	SM-9.5E	5.8	2.3	7.1	14.9	19.1	84.6	62.7
D-FL	SM-9.5A	6.3	1.3	5.3	14.9	18.4	91.2	71.3
E-FL	SM-9.5D	5.9	1.4	7.3	13.2	18.5	89.6	60.4
F-FL	SM-9.5D	5.4	3.6	8.2	14.5	18.6	75.4	56.2
G-FL	SM-9.5D	6.3	3.6	9.0	16.6	21.3	78.6	57.8
H-FL	SM-9.5D	5.6	4.1	8.7	15.6	19.6	73.4	55.7
I-FL	SM-9.5A *	5.4	1.5	6.4	13.2	17.5	88.5	63.8
J-FL	SM-9.5D	4.9	7.5	11.2	16.9	20.3	55.5	44.6
L-FL	SMA-12.5	6.8	1.8	7.9	16.4	21.6	89.0	65.4

* Designed using high laboratory compaction.

Table 8. Volumetric properties of L/L samples.

Section	Mix	Asphalt (%)	VTM (%)		VMA (%)		VFA (%)	
			Gyratory	Vibratory	Gyratory	Vibratory	Gyratory	Vibratory
A-LL	SM-12.5D	5.9	5.2	11.0	18.1	23.5	71.4	53.2
B-LL	SM-9.5D	5.4	1.8	7.9	12.9	18.3	86.0	56.8
C-LL	SM-9.5E	6.0	2.0	8.9	15.3	21.2	86.6	58.1
D-LL	SM-9.5A	6.8	0.9	8.4	15.8	22.2	94.4	62.2
E-H-LL	SM-9.5D	6.0	1.9	8.3	14.4	20.0	86.8	58.5
I-LL	SM-9.5A *	5.3	6.0	10.2	17.0	20.7	64.8	50.7
J-LL	SM-9.5D	5.1	4.6	10.7	14.7	20.2	68.6	46.9

* Designed using high laboratory compaction.

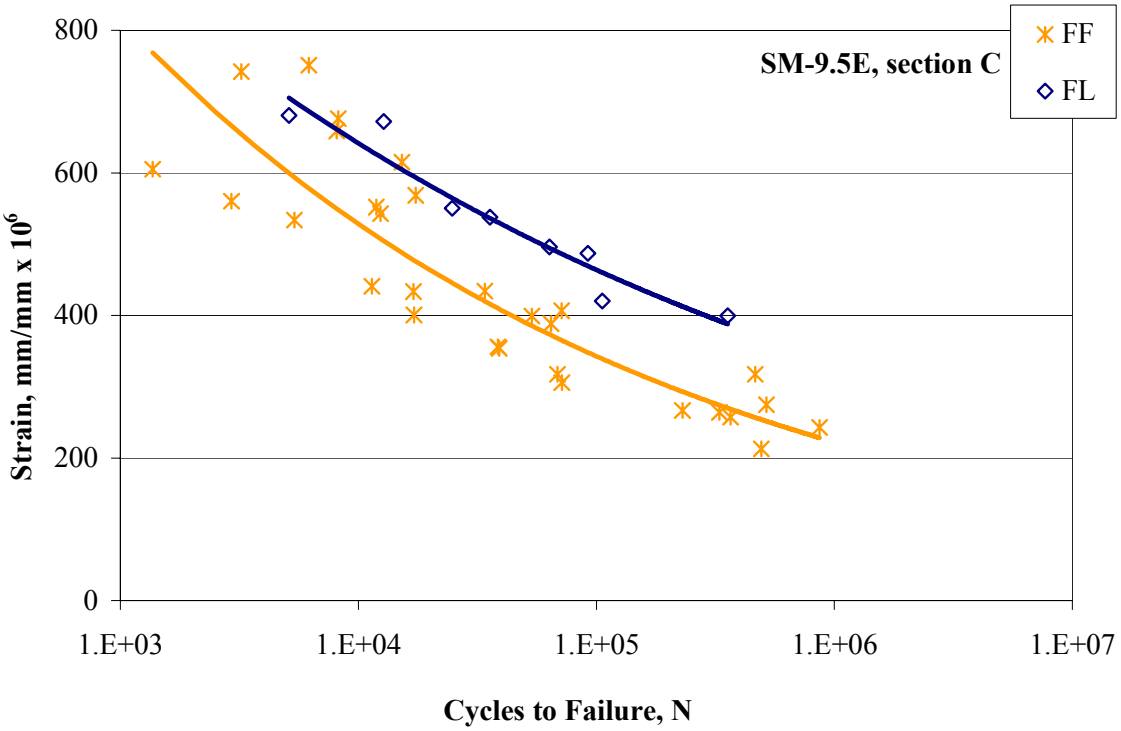

Figure 5. Comparison of field and laboratory compaction effects for SM-9.5E, section C.

problem may be resolved by increasing the lateral size of the vibratory compaction mold used such that the mixture is able to more freely move under compaction; this would require fatigue beams to be saw-cut to size for testing rather than tested without cutting as was done in this study.

To evaluate the difference between production and compaction in the field and in the laboratory, four mix types were utilized in this study: F/F, F/L, L/L, and D/L. The designations were discussed previously. Comparison of F/F and F/L samples is indicative of differences in performance and properties due to compaction, as the F/F samples are saw-cut from the pavement while the F/L samples are compacted in the laboratory from field –produced loose HMA samples. Comparison of F/L and L/L samples is indicative of differences in performance and properties due to production as F/L samples were produced in the field and L/L samples were produced in the laboratory; both sample sets were compacted in the laboratory. Comparison of the L/L and D/L samples indicates the changes in performance expected when differences are seen between the in-situ HMA and the job mix formula.

By comparing the F/F and F/L mixes, the difference in properties and performance due to compaction may be evaluated; this evaluation was performed using samples of SM-9.5E, section C. Strain versus fatigue life (S-N) curves are shown for the F/F and F/L samples in Figure 5. From this figure, it is clear that there is a difference between the F/F and F/L samples. It is also clear that there is a much greater variability in the F/F samples. In part, this is because the F/F

samples shown are from three locations within the lane and were cut using two orientations. This demonstrates that the variability inherent in the vibratory compaction process is less than that found from in-situ compaction.

The comparison of the F/L and L/L samples is indicative of differences in fatigue life due to preparation methods. Comparison of L/L and D/L samples indicate the importance of meeting the job mix formula. Figures 5 through 10 show comparisons of the different production and compaction combinations on fatigue life for each mixture. The equation coefficients for the trend line seen for each sample set were previously presented in Table 4.

Considering Figure 6, showing results for the SM-9.5A mixture from section D, it is shown that the L/L and D/L samples were very similar in fatigue response. The volumetric analysis for these mixtures indicated that there was no significant difference in the mixtures; as the L/L mixture was produced in the laboratory from the F/L material analysis results, it indicates that there were no differences between the mixture placed in the field and the JMF. The clear difference between the F/L samples and the L/L samples indicates a significant difference in the preparation between the laboratory and the batch plant. This difference is seen in all of the 9.5 mm nominal maximum aggregate sized mixtures; however, this trend does not necessarily imply an aggregate dependence to the difference, since only one 12.5 mm nominal maximum aggregate mixture was fully evaluated in this study.

The fatigue performance of the SM-9.5D mixture located in section B is seen in Figure 7. The performance of the F/L samples is suspect in this figure, as the volumetric properties of these

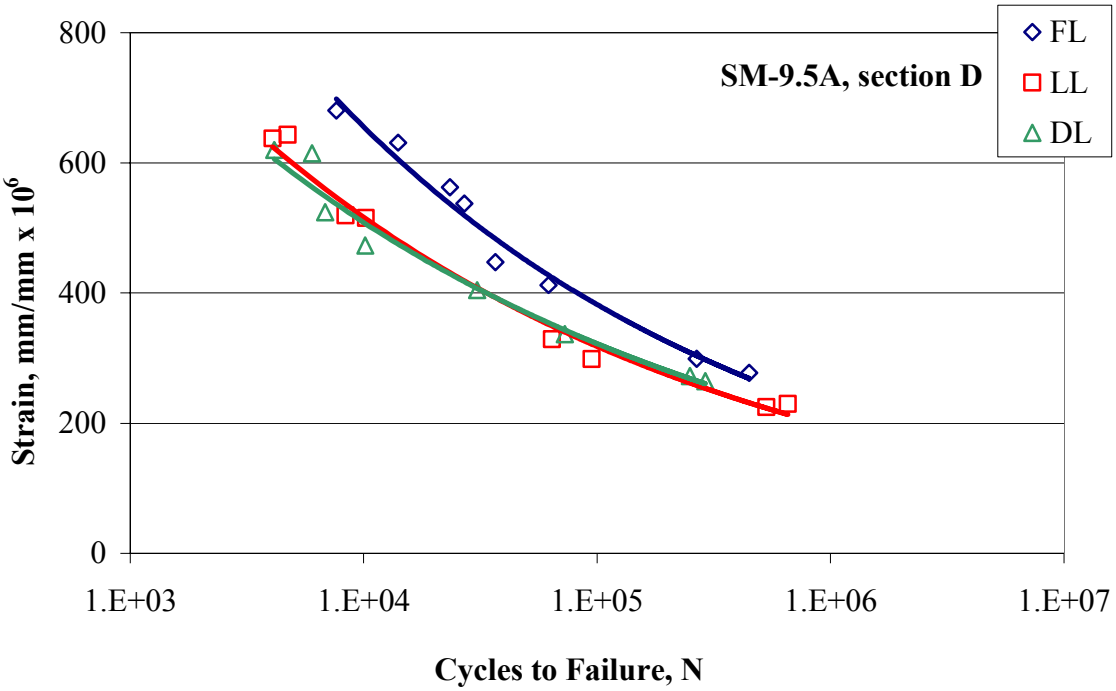

Figure 6. Comparison of production method for SM-9.5A, section D.

samples indicated that the bagged samples had a lower asphalt content and a higher air content than expected; overall, the result was a greater variability during fatigue testing and a unique response when compared with the L/L and D/L results. Figure 7 indicates that the F/L mixture is better-performing under high strain conditions but that increased deterioration is seen at relatively low strains. In contrast to the unusual response seen in the F/L mixture, the L/L and D/L responses are consistent; the D/L mixture is shown to perform better than the L/L mixture that was replicated in the laboratory from the field material properties.

Figure 8 illustrates the performance of the SM-9.5E mixture found in section C. This mixture contains a PG76-22 polymer-modified binder and is expected to perform well in fatigue analysis due to the polymer content. Difficulties were experienced during the laboratory compaction of the SM-9.5E due to the polymer content and its effect on the mixture properties during mixing and compaction. These difficulties resulted in a slightly higher VTM than desired and may have affected the fatigue life of these samples. The F/L mixture performed best across the strain range seen in this study; however, the L/L mixture indicates an improved response at higher strains. The D/L samples performed better than the L/L samples, and the trend appears to be shifted vertically from that of the F/L samples.

The fatigue response of the SM-12.5D mixture found in section A is shown in Figure 9. This figure indicates that for this mixture, there were no significant differences between the batch-plant and laboratory production methods, nor were there significant differences between the L/L and D/L mixtures in terms of performance.

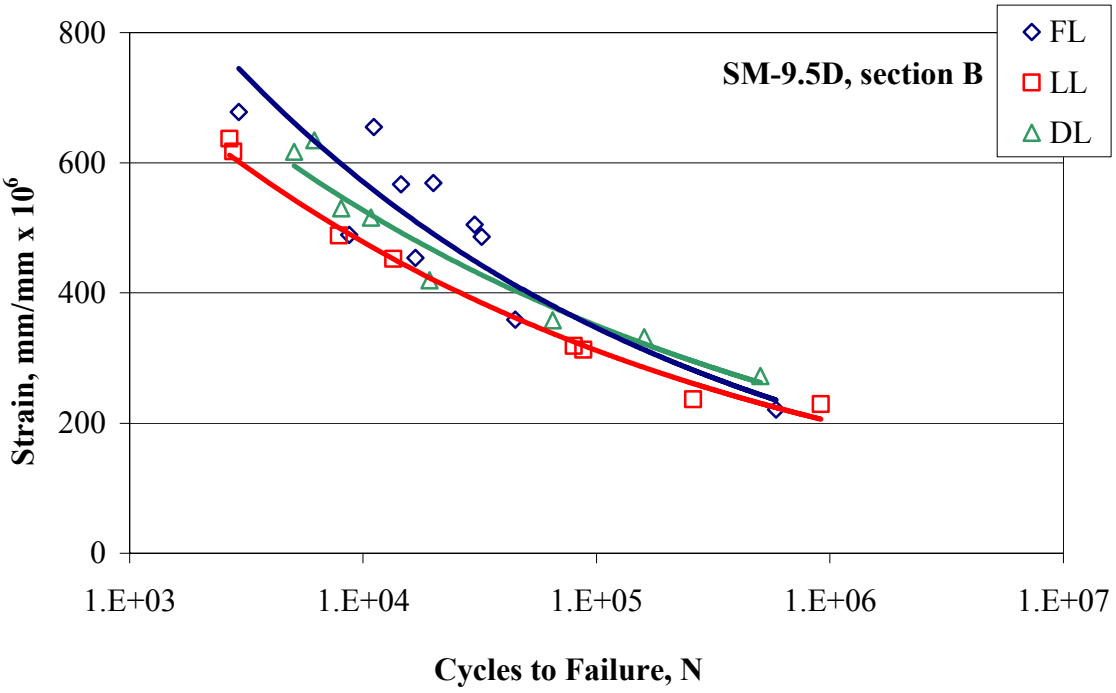

Figure 7. Comparison of production methods for SM-9.5D, section B.

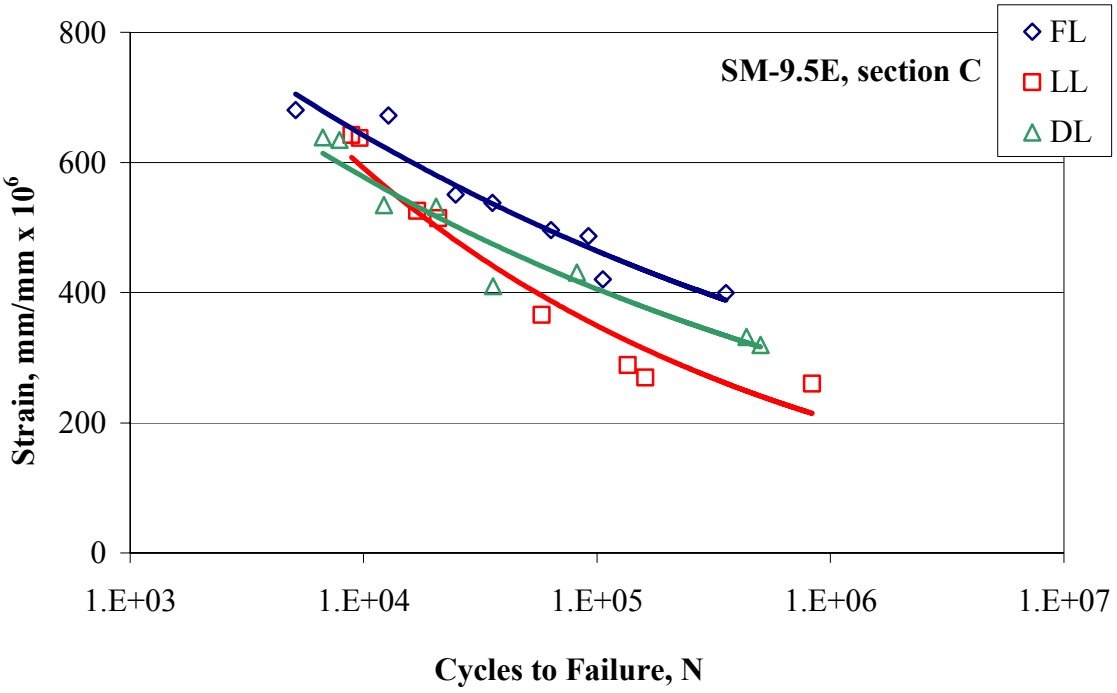

Figure 8. Comparison of production methods for SM-9.5E, section C.

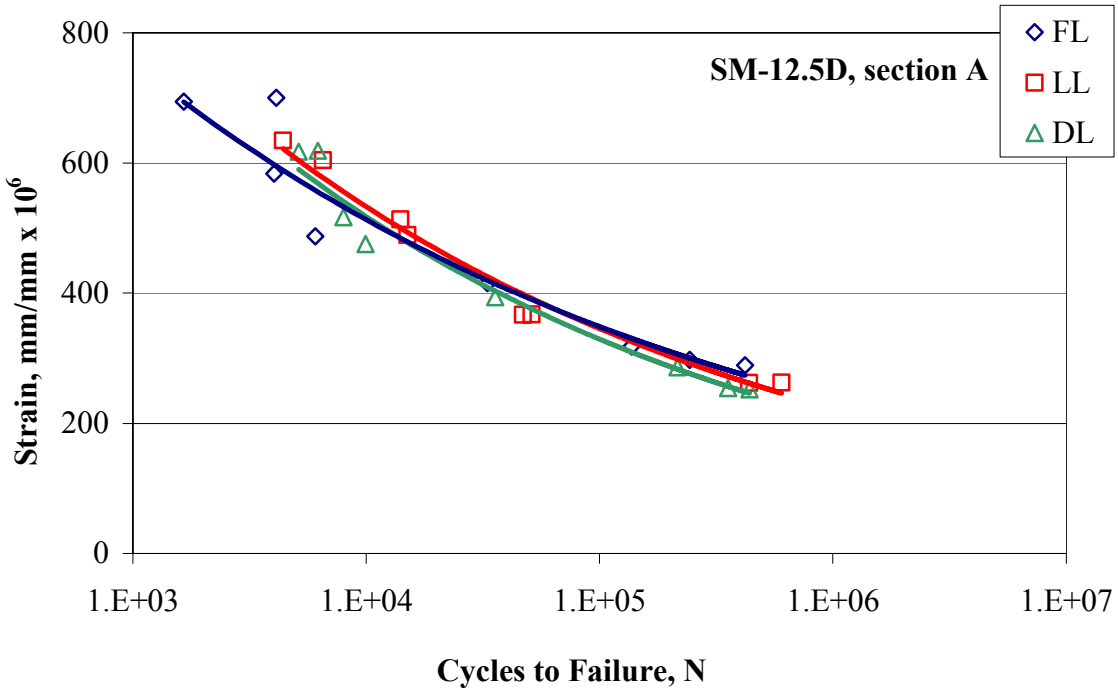

Figure 9. Comparison of production methods for SM-12.5D, section A.

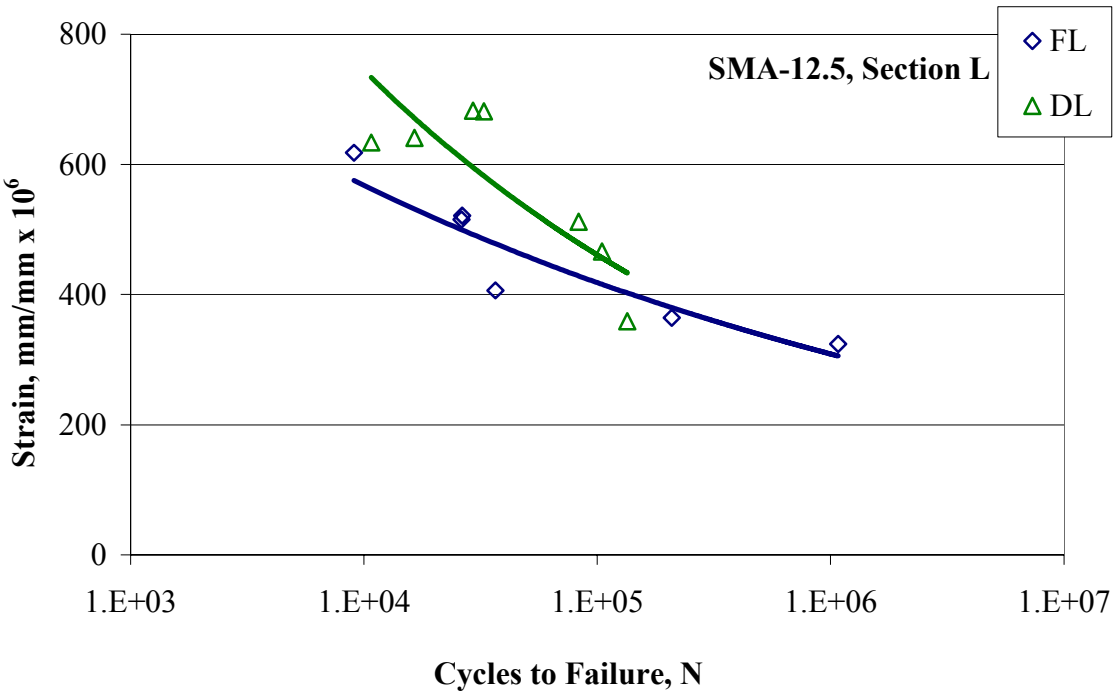

Figure 10. Comparison of production methods for SMA-12.5, section L.

Figure 10 displays the fatigue performance of the SMA-12.5 mixture found in section L. This mixture was only produced as F/L and D/L mixtures due to the difficulty in obtaining the required aggregate. Additionally, difficulties were experienced during both mixing and compaction of the mixture due to the fiber additives. As a result, both the F/L and D/L results show a very high variability in sample responses. This is more pronounced in the D/L samples due to the difficulties encountered during laboratory production of the mixture, which included sensitivity to mixing and compaction temperature and a tendency for the fibers to "clump" during mixing. It is assumed that these difficulties were not present during batch production. In general, considering the variability in response, the fatigue performance of the SMA-12.5 is not conclusive; however, there is indication of improved fatigue resistance in the F/L response that justifies further investigation of this mixture.

Figure 11 illustrates the differences in the SM-9.5A mixture from section I; this section was designed using a higher level of laboratory compaction and has a lower VTM than does the mixture in section D. This figure continues the trend in which the batch-plant produced mixture performs better in fatigue analysis than does the laboratory-produced mixture across the tested range of strains; however, in considering the trends shown in the figure, it appears that the L/L and D/L mixtures will perform better at higher strains (outside the scope of this study) than the F/L mixture. The discrepancies between the mixture as produced and the JMF appear to have improved the fatigue performance of the mixture under the given compaction.

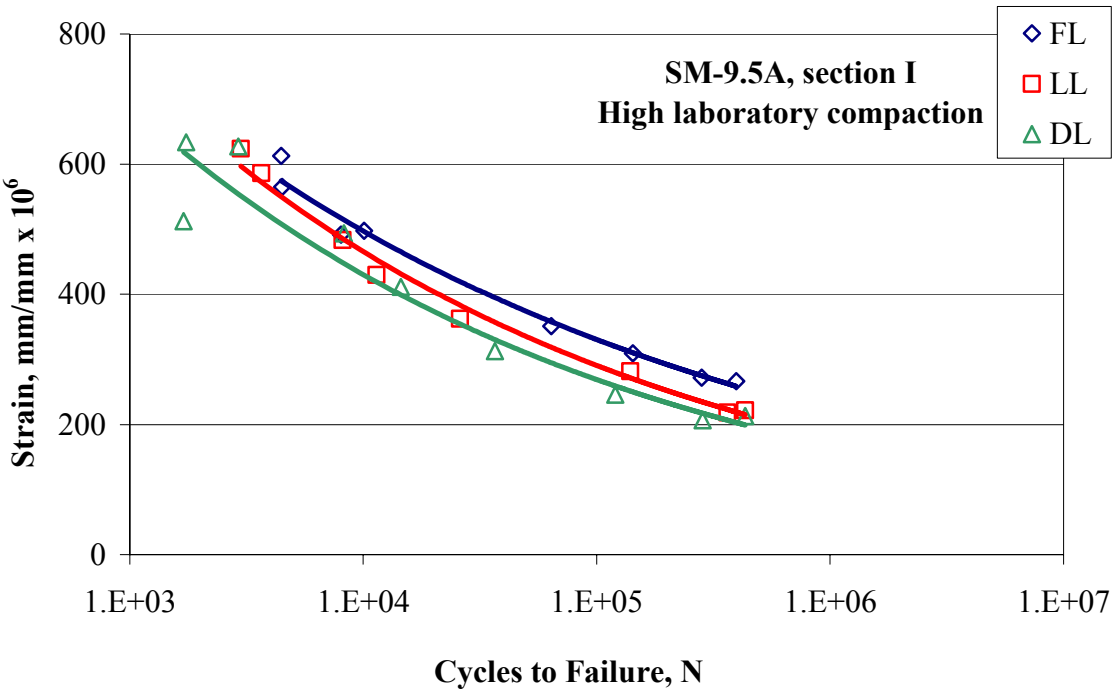

Figure 11. Comparison of production method for SM-9.5A, section I, high laboratory compaction.

Evaluation of Aggregate and Binder Effects

Comparisons were performed to evaluate the effects of aggregate size and binder type on fatigue performance during laboratory testing. Figure 12 shows the results of the aggregate analysis. The two mixtures shown, SM-12.5D and SM9.5D, were produced using the same PG70-22 binder and having maximum nominal aggregate sizes of 12.5mm and 9.5mm respectively. As can be seen in the figure, the effect of the differing aggregate sizes on the fatigue performance is inconclusive and cannot be separated form the production or compaction method considering the samples available to this study.

Figures 13 through 15 show the fatigue response of mixtures containing the three binders used in this study. The binders used included PG64-22, PG70-22, and PG76-22 polymer-modified. It can be seen in Figures 13 through 15 that the polymer-modified PG76-22 performs best for all production/compaction combinations. The results indicate that for the F/L and L/L mixtures, the PG70-22 performs less well compared to the PG64-22; however for the D/L samples produced according to the JMF, the PG70-22 performed slightly better than the PG64-22. The response seen for the PG64-22 and PG70-22 may be influenced by the binder contents of the mixes: in every case the binder content of PG64-22 is greater than the contents of the PG70-22. The binder type response may be obscured in this situation by the effect of binder content. The effects of the PG76-22 polymer-modified binder on fatigue life are great enough that they are observed even though the binder content of the SM9.5E mixes is, in all cases other than the F/L, less than that of either the SM9.5A or SM-9.5D mixtures.

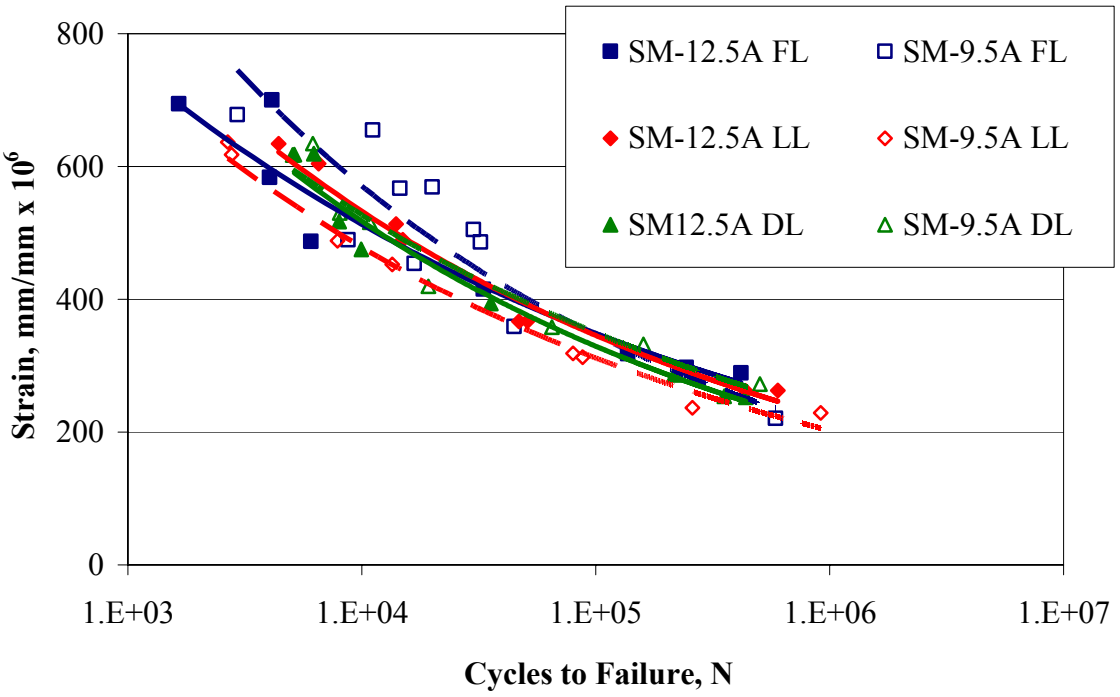

Figure 12. Effects of aggregate size on laboratory fatigue life.

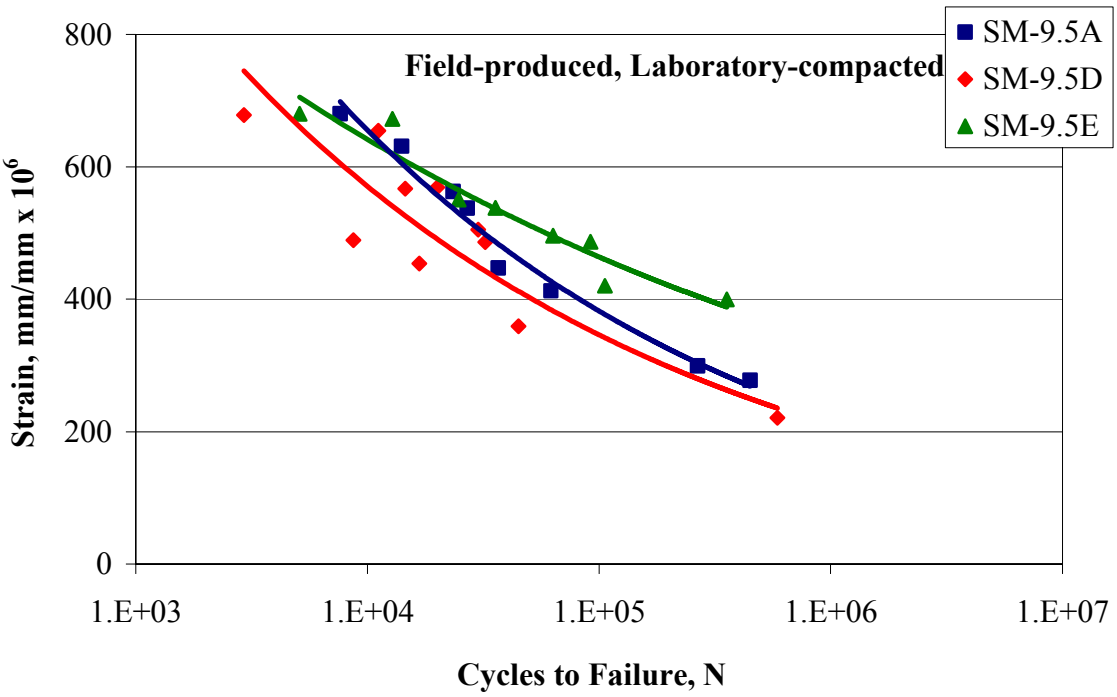

Figure 13. Comparison of binder effects on fatigue life, field-produced, laboratory-compacted mixtures.

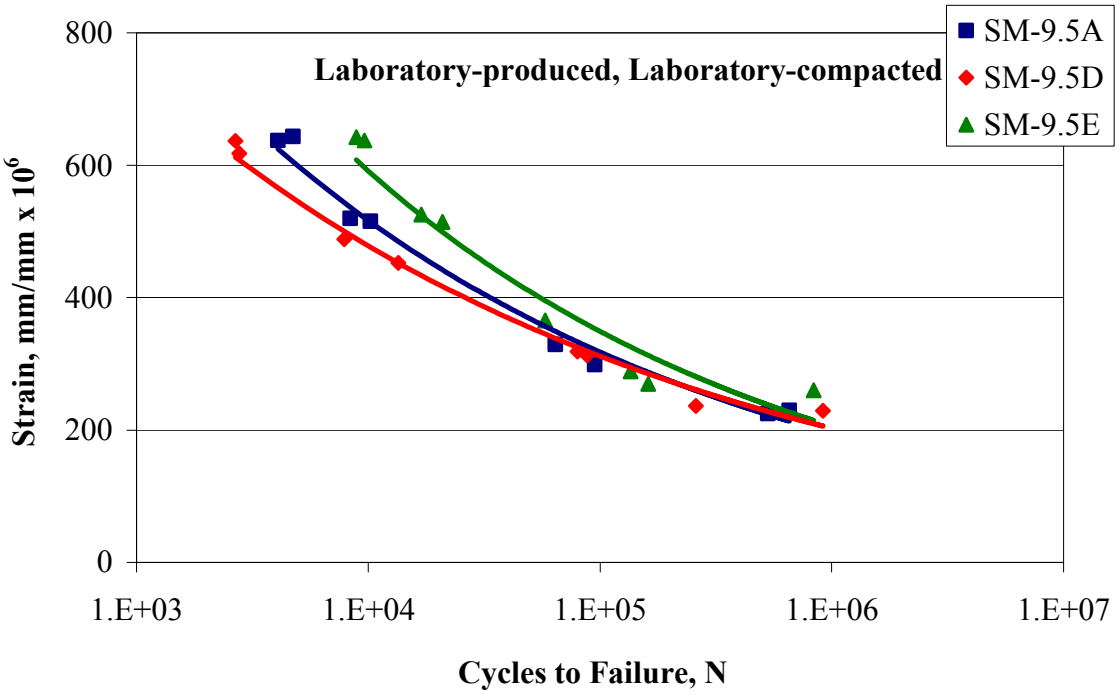

Figure 14. Comparison of binder effects on fatigue life, laboratory-produced, laboratory-compacted mixtures.

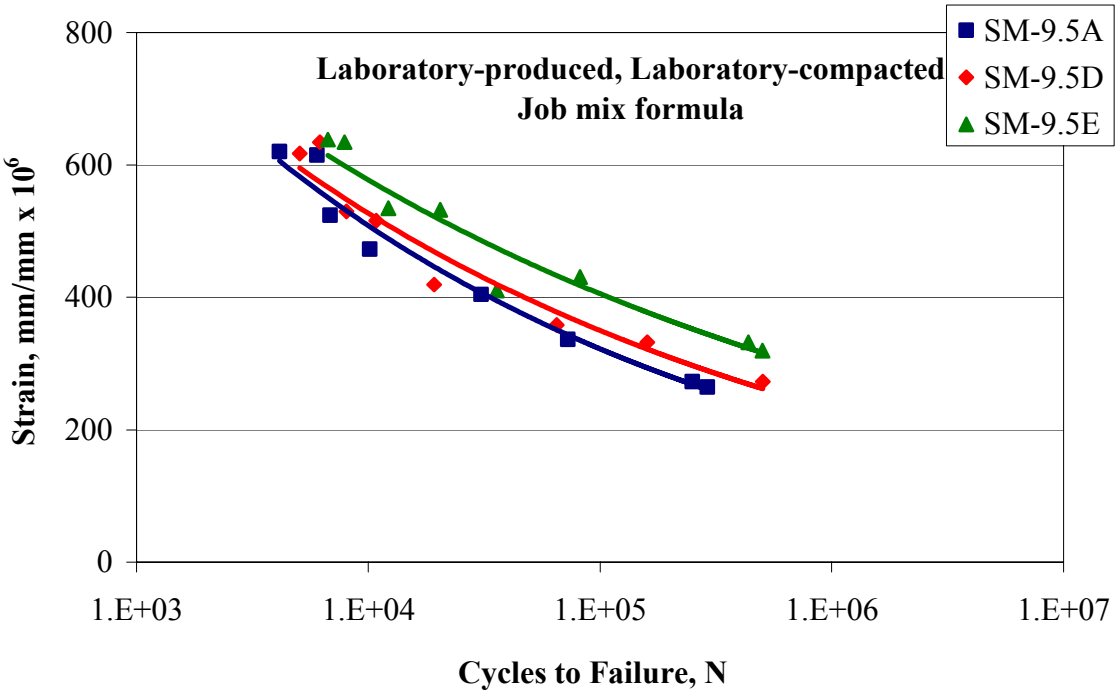

Figure 15. Comparison of binder effects on fatigue life, laboratory-produced, laboratory-compacted mixtures using JMF.

The coefficients seen in Table 4 for equation 8 were used to predict the fatigue life for each tested mixture under each production/compaction scenario at five strains ranging from 200 to 1000 microstrain. The resulting comparisons are shown in Figures 16 through 18.

Figure 16 shows the predicted fatigue lives for the field-mixed, laboratory-compacted mixtures. This figure indicates the F/L mixtures may have different rankings in terms of fatigue response at different applied strains. At high strains, 800 microstrain and above, the SM-9.5A and SM-9.5D (located in section B) mixtures showed the best resistance to fatigue; however at lower strains, the SM-9.5E mixture indicated a superior performance.

The predicted fatigue lives for the L/L mixtures are shown in Figure 17. This figure indicates that there are few differences in the predicted fatigue lives for all laboratory-produced and –compacted mixtures. At strains above 500 microstrain, the SM-9.5E indicates a better resistance to fatigue.

D/L mixture predicted fatigue lives are compared in Figure 18. This figure indicates that overall, the SMA-12.5 may have the best fatigue resistance, based on laboratory design mixtures. The next best performance is shown by the SM-9.5E mixture. These results indicate the benefits to fatigue life that can be seen through the use of fiber-modification of mixes or polymer

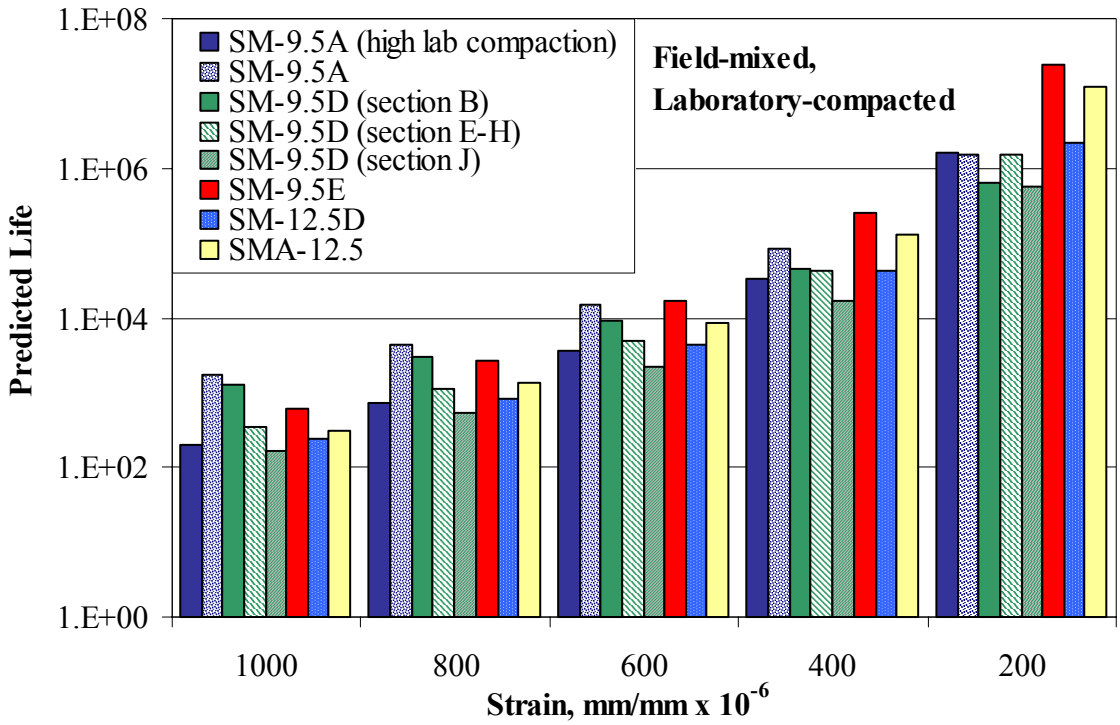

Figure 16. Effect of binder type on predicted fatigue life; field-mixed, laboratory-compacted mixtures.

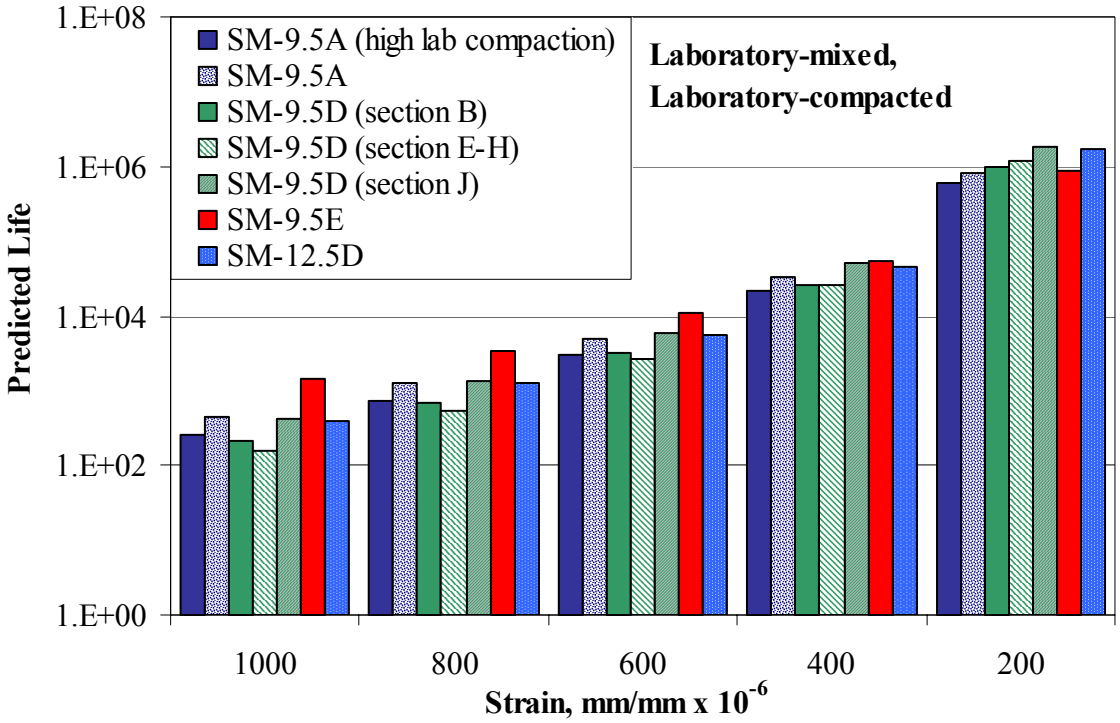

Figure 17. Effect of binder type on predicted fatigue life, laboratory-mixed, laboratory-compacted mixtures.

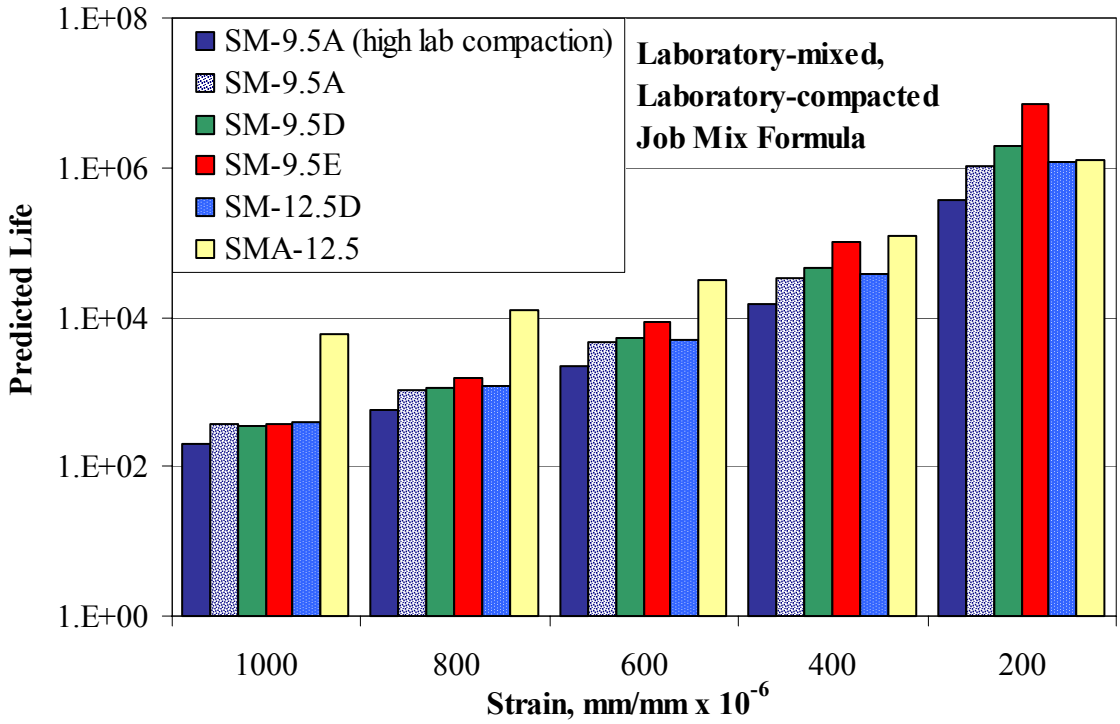

Figure 18. Effect of binder type on predicted fatigue life, laboratory-mixed, laboratory-compacted JMF mixtures.

modification of binders; however, these mixes were optimized only in the laboratory. The results shown for the F/L and L/L mixtures indicate that mixtures produced for placement in the field may not have the idealized properties of those indicated by the job mix formula and designed in the laboratory.

CONCLUSIONS

Fatigue testing of Superpave surface mixtures in use at the Virginia Smart Road was performed for mixture characterization and evaluation purposes. The response of the mixtures in fatigue testing and equations relating applied strain and resulting fatigue life were presented. Evaluation of the effects on laboratory fatigue life of specimen location and orientation within the pavement surface was performed. Differences between field and laboratory production and compaction were discussed and their effect on mixture fatigue resistance was considered. The effects of aggregate size and binder type on fatigue life were determined. Finally, the fatigue responses of the tested mixtures were compared and differences in the predicted fatigue life were evaluated.

Considering the responses from the mixtures evaluated in this study, it can be concluded that batch-plant production has a significant impact on fatigue performance, most likely due to the reduction of variability inherent in a large-batch process as compared to the lesser volumes produced in laboratory batches. In every case except that of the SMA-12.5 mixture, the batch-plant produced mixtures performed better than or equivalent to the laboratory produced mixtures. The differences between the D/L mixtures produced according to the JMF and the L/L mixtures produced to emulate the field mixtures were less well-defined. In all cases except the SM-9.5A mixture designed with high laboratory compaction, the D/L mixture performed consistently better than or equivalent to the L/L mixture during laboratory fatigue testing. This comparison simply indicates that JMF mixtures are well designed; the conclusion of best-performing mixture type is subjective at best and not well supported given the sample pool in this study.

The effect of the differing aggregate sizes on fatigue was found to be inconclusive and was not able to be separated from production or compaction effects for the samples in this study. Binder evaluation indicated that, for mixes produced according to the JMF, polymer modification resulted in improvements to fatigue life. Overall comparison of the mixtures indicated mixed performance. Predicted fatigue lives for each mixture indicated that use of polymer-modification or SMA mixtures enhanced fatigue performance when the mixtures were produced according tot eh job mix formula; deviations from the JMF appeared to adversely affect predicted fatigue performance.

Results from the fatigue evaluation allowed verification of several hypotheses related to mixture production and compaction and fatigue performance with respect to the mixtures evaluated in this study. The following findings are presented:

1. Mixtures incorporating fiber additives or polymer-modified binders are significantly more difficult to produce in the laboratory and are prone to inherent errors due to the difficulty of material handling during production and compaction.

2. Location within the pavement surface (wheelpath or center-of-lane) does not significantly affect laboratory fatigue test results, although the location will have significant effects on in-situ fatigue life.

3. Orientation of cut samples (parallel or perpendicular to the direction of traffic) has a minor effect on the laboratory fatigue life; the variability inherent in the pavement due to material variability is greater than the variability induced by direction of compaction.

4. The vibratory compactor was found to be an acceptable alternative for compaction of slab samples; however, it required careful adjustment to produce specimens with consistent properties. The mold size was found to be important in the replication of in-situ properties, especially for large aggregate mixtures and mixtures having low VTM.

5. Fatigue life of laboratory-compacted samples was found to be greater than fatigue life of field-compacted samples for the SM-9.5E mixture evaluated during this study; additionally, the test variability of the laboratory-compacted mixture was less than that of the field-compacted mixture.

6. Batch-plant production significantly reduces specimen variability as compared to small-batch production in the laboratory when the same compaction is used on both specimen sets.

In Smart Road mixtures produced according to the job mix formula, the use of polymer-modified binder or SMA mixtures was shown to increase the expected fatigue life. However, results for all mixes indicated that fatigue resistance rankings may change depending on the applied strain level. All results of this study are applicable only to the surface mixtures tested in the study and cannot be generalized to other VDOT or Superpave mixtures without verification testing.

RECOMMENDATIONS

Testing was performed on variations of six Superpave mixtures having specific properties. Additional testing using controlled changes in mixture properties such as asphalt content and VTM for each mixture should be performed to fully quantify the effects of these variables and to evaluate the dependence of fatigue life on volumetric properties. Additional testing on samples cut from the in-situ pavement should be evaluated to verify the results obtained herein regarding specimen orientation and in-situ mixture variability. Fatigue evaluation of mixtures at different temperatures should be performed to characterize and quantify the temperature susceptibility of these mixtures under fatigue loading. Testing should also be performed on the asphalt base mixtures to evaluate their fatigue properties and contributions to the overall pavement fatigue response.

Additional analysis should be performed to further evaluate the ability of the vibratory compactor to replicate in-situ material volumetric properties. The consideration of differing mold capacities and the effects on the resulting volumetric properties should be evaluated, as should the effect of using un-cut as-compacted specimens versus specimens cut from larger slabs. Since specimens cut from the in-situ pavement have different surface conditions from the specimens utilized in this study, assessment should be made of the significance of such effects.

Finally, application of the presented fatigue life models to pavement designs should be performed by comparing the fatigue response from the laboratory testing with observed fatigue development in in-situ pavements. This should result in quantifiable response model to explain the discrepancies seen between laboratory fatigue and in-situ pavement fatigue.

COST AND BENEFIT ASSESSMENT

This study contributes to the understanding of the factors involved in fatigue performance of asphalt mixtures. Improved material performance has a direct correlation with improved pavement performance, resulting in reduced maintenance needs and longer service lives of pavements. Considering that approximately 95% of Virginia's interstate and primary roadways incorporate asphalt surface mixtures, and that fatigue is a leading cause of deterioration, gains in the understanding of fatigue processes and prevention have great potential payoff by improving both the mixture and pavement design practices.

REFERENCES

Adedimila, A. S. and T. W. Kennedy. (1976) Repeated-Load Indirect Tensile Fatigue Characteristics of Asphalt Mixtures. Transportation Research Record, no. 595, Transportation Research Board, Washington, DC, pp. 25-33.

Asphalt Institute. (1996) Superpave Mix Design. Superpave Series No. 2, Asphalt Institute, Lexington, KY, 117p.

Baladi, G. Y., R. S. Harichandran, and R. W. Lyles. (1988) New Relationship between Structural Properties and Asphalt Mix Parameters. Transportation Research Record, no. 1171, Transportation Research Board, Washington, DC, pp. 168-177.

Balbissi, A. H. (1983) A Comparative Analysis of the Fracture and Fatigue Properties of Asphalt Concrete and Sulphlex. PhD thesis, Texas A&M University, College Station, TX.

Bell, C. A., R. G. Hicks, and J. E. Wilson. (1984) Effect of Percent Compaction on Asphalt Mixture Life. ASTM Special Technical Publication, no. 829, ASTM, Philadelphia, Pa, pp. 107-130.

Brennan, M. J., J. Meade, M. Hynes, D. J. Murphy, and C. Lycett. (1996) A Pilot Study of the Performance of Porous Asphalt in Static Creep and Repeated Loading. Proceedings of the Eurasphalt and Eurobitume Congress, Strasbourg, France.

Button, J. W., D. N. Little, V. Jagadam, and O. J. Pendleton. (1994) Correlation of Selected Laboratory Compaction Methods with Field Compaction. Transportation Research Record, no. 1454, Transportation Research Board, Washington, DC, pp. 193-201.

Collop, A. C. and D. Cebon. (1995) Theoretical analysis of fatigue cracking in flexible pavements. Proceedings of the Institution of Mechanical Engineers Part C-Journal of Mechanical Engineering Science, vol. 209, no. 5, pp. 345-361.

Consuegra, A., D. N. Little, H. Von Quintus, and J. Burati. (1989) Comparative Evaluation of Laboratory Compaction Devices Based on Their Ability to Produce Mixtures with Engineering Properties Similar to Those Produced in the Field. Transportation Research Record, no. 1228, Transportation Research Board, Washington DC, pp. 80-87.

Deacon, J. A., J. S. Coplantz, A. A. Tayebali, and C. L. Monismith. (1994) Temperature Considerations in Asphalt-Aggregate Mixture Analysis and Design. Transportation Research Record, no. 1454, pp. 97-112.

Deacon, J. A., A. A. Tayebali, G. M. Rowe, and C. L. Monismith. (1995a) Validation of SHRP A-003A flexural beam fatigue test. ASTM Special Technical Publication, no. 1265, ASTM, Philadelphia, PA, pp. 21-36.

Deacon, J. A., R. B. Leahy, and C. L. Monismith. (1995b) Mix Testing and Analysis Systems Resulting from SHRP Contract A-003A. Transportation Congress, Proceedings, vol. 1, ASCE, New York, NY, pp. 691-711.

Francken, L. and J. Verstraeten. (1974) Methods for Predicting Moduli and Fatigue laws of Bituminous Road Mixtures under Repeated Bending. Transportation Research Record, no. 515, Transportation Research Board, Washington, DC, pp. 114-123.

Ghuzlan, K. and S. H. Carpenter. (2000) An Energy-Derived / Damage-Based Failure Criteria for Fatigue Testing. Transportation Research Record, no. 1723, Transportation Research Board, Washington, DC, pp. 141-149.

Harvey, J. and C. L. Monismith. (1993) Effects of Laboratory Asphalt Concrete Specimen Preparation Variables on Fatigue and Permanent Deformation Test Results Using Strategic Highway Research Program A-003A Proposed Testing Equipment. Transportation Research Record, no. 1417, Transportation Research Board, Washington, DC, pp. 38-48.

Harvey, J., T. Lee, J. Sousa, J. Pak, and C. L. Monismith. (1994) Evaluation of Fatigue and Permanent Deformation Properties of Several Asphalt-Aggregate Field Mixes Using

Strategic Highway Research Program A-003A Equipment. Transportation Research Record, no. 1454, Transportation Research Board, Washington, DC, pp. 123-133.

Harvey, J. T. and B. Tsai. (1996) Effects of Asphalt Content and Air Void Content on Mix Fatigue and Stiffness. Transportation Research Record, no. 1543, Transportation Research Board, Washington, DC, pp. 38-45.

Hveem, F. N. and R. M. Carmany. (1948) The Factors Underlying the Rational Design of Pavements. Proceedings of the Highway Research Board, vol. 28, Highway Research Board, Washington, DC, pp. 101-136.

Irwin, L. H. and B. M. Gallaway. (1974) Influence of Laboratory Test Method on Fatigue Test Results for Asphaltic Concrete. ASTM Special Technical Publication 561, American Society for Testing and Materials, Philadelphia, PA, pp. 12-46.

Khalid, H. A. (2000a) Comparison between Bending and Diametral Fatigue Tests for Bituminous Materials. Materials & Structures, vol. 33, no. 231, pp. 457-465.

Khalid, H A. (2000b) Evaluation of Asphalt Fatigue Properties in the Laboratory. Proceedings of the Institution of Civil Engineers-Transport, vol. 141, no. 4, pp. 171-178.

Khan, Z. A., H. I. Al-Abdul, I. Asi, R. Ramadhan. (1998) Comparative Study of Asphalt Concrete Laboratory Compaction Methods to Simulate Field Compaction. Construction and Building Materials, vol. 12, no. 6-7, pp. 373-384.

Khedaywi, T. S. and T. D. White. (1996) Effect of Segregation on Fatigue Performance of Asphalt Paving Mixtures. Transportation Research Record, no. 1543, Transportation Research Board, Washington, DC, pp. 63-70.

Kim, Y. R., N. Kim, and N. P. Khosla. (1992) Effects of Aggregate Type and Gradation on Fatigue and Permanent Deformation of Asphalt Concrete. ASTM Special Technical Publication, no. 1147, ASTM, Philadelphia, PA, pp. 310-328.

Kim, Y. R., H.-J. Lee, and D. N. Little. (1997) Fatigue Characterization of Asphalt Concrete Using Viscoelasticity and Continuum Damage Theory. Journal of the Association of Asphalt Paving Technologists, vol. 66, pp. 521-569.

Leahy, R. B., C. L. Monismith, and J. R. Lundy. (1995) Performance-based Properties of Asphalt Concrete Mixes. ASTM Special Technical Publication, no. 1265, ASTM, Philadelphia, PA, pp. 37-54.

Little, D. N., R. L. Lytton, D. Williams, and C. W. Chen. (2001) Microdamage Healing in Asphalt and Asphalt Concrete, Volume I: Microdamage and Microdamage Healing, Project Summary Report. Research Report FHWA-RD-98-141, Federal Highway Administration, McLean, VA.

Majidzadeh, K., E. M. Kauffman, and C. W. Chang. (1973) Verification of Fracture Mechanics Concepts to Predict Fatigue Cracking in Pavements. Report No. FHWA-RD-73-91, Federal Highway Administration, Washington, DC.

Masad, E., S. Muhunthan, N Shashidhar, and T. Harman. (1999) Quantifying Laboratory Compaction Effects on the Internal Structure of Asphalt Concrete. Transportation Research Record, no. 1681, Transportation Research Board, Washington, DC, pp. 179-185.

Matthews, J. M. and C. L. Monismith. (1993) Direct Tension and Simple Stiffness Tests. Tools for the Fatigue Design of Asphalt Concrete Layers. Transportation Research Record, no. 1388, Transportation Research Board, Washington, DC, pp. 182-199.

Matthews, J. M., C. L Monismith, and J. Craus. (1993) Investigation of Laboratory Fatigue Testing Procedures for Asphalt Aggregate Mixtures. Journal of Transportation Engineering, vol. 119, no. 4, pp. 634-654.

Maupin, G. W. (1972) Results of Indirect Tensile Tests Related to Asphalt Fatigue. Highway Research Record, no. 404, Highway Research Board, Washington, DC, pp. 1-7.

Maupin, G. W. (1977) Test for Predicting Fatigue Life of Bituminous Concrete. Transportation Research Record, no. 659, Transportation Research Board, Washington, DC, pp. 32-37.

Monismith, C. L. and J. A. Deacon. (1969) Fatigue of Asphalt Paving Mixtures. ASCE Transportation Engineering Journal, vol. 95, no. 2, pp. 317-346.

Monismith, C. L. (1981) Fatigue Characteristics of Asphalt Paving Mixtures and Their Use in Pavement Design. Proceedings of the 18th Paving Conference, University of New Mexico, Albuquerque, NM, pp. 1-43.

Pell, P. S. and K. E. Cooper. (1975) The Effect of Testing and Mix Variables on the Fatigue Performance of Bituminous Materials. Proceedings of the Association of Asphalt Paving Technologists, vol. 44, pp. 1-37.

Pronk, A. C. (1997) Comparison of 2 and 4 Point Fatigue Tests and Healing in a 4 Point Dynamic Bending Test Based on the Dissipated Energy Concept. Proceedings, Eighth International Conference on Asphalt Pavements, vol. 2, Seattle, WA, pp. 986-994.

Radziszewski, P. (1997) Fatigue Characteristics of Asphalt Modified Paving Mixtures and their Use in Pavement Design. Archives of Civil Engineering, vol. 43, no. 2, pp. 199-215.

Ramsamooj, D V. (1991) Prediction of Fatigue Life of Asphalt Concrete Beams from Fracture Tests. Journal of Testing & Evaluation, vol. 19, no. 3, pp. 231-239.

Ramsamooj, D. V. (1980) Fatigue Cracking of Asphalt Pavements. Transportation Research Record, no. 756, Transportation Research Record, Washington, DC, pp. 43-48.

Read, J. M. and S. F. Brown. (1996) Practical Evaluation of Fatigue Strength for Bituminous Mixtures. Proceedings of the Eurasphalt and Eurobitume Congress, Strasbourg, France.

Read, J. M. and A. C. Collop. (1997) Practical Fatigue Characterization of Bituminous Paving Mixtures. Journal of the Association of Asphalt Paving Technologists, vol. 66, pp. 74-108.

Roberts, F. L., P. S. Kandhal, E. R. Brown, D.-Y. Lee, and T. W. Kennedy. (1996) Hot Mix Asphalt Materials, Mixture Design, and Construction. NAPA Research and Education Foundation, Lanham, MD, 585p.

SHRP. (1994) Fatigue Response of Asphalt-Aggregate Mixes. Report SHRP-A-404, Strategic Highway Research Program, National Research Council, Washington, DC, 309p.

Sousa, J. B., J. C. Pais, M. Prates, R. Barros, P. Langlois, and A.-M. Leclerc. (1998) Effect of Aggregate Gradation on Fatigue Life of Asphalt Concrete Mixes. Transportation Research Record, no. 1630, Transportation Research Board, Washington, DC, pp. 62-68.

Tayebali, A., G. Rowe, and J. Sousa. (1992) Fatigue Response of Aggregate-Asphalt Mixtures. Journal of the Association of Asphalt Paving Technologists, vol. 61, pp. 333-360.

Tayebali, A., J. Deacon, J. Coplantz, J. Harvey, and C. Monismith. (1994) Mixture and Mode-of-Loading Effects on Fatigue Response of Asphalt-Aggregate Mixtures. Journal of the Association of Asphalt Paving Technologists, vol. 63, pp. 118-151.

Tayebali, A. A., J. A. Deacon, and C. L. Monismith. (1996a) Development and Evaluation of Surrogate Fatigue Models for SHRP A-300A Abridged Mix Design Procedure. Proceedings of the Association of Asphalt Paving Technologists, vol. 64, pp. 340-366.

Tayebali, A. A., J. A. Deacon, and C. L. Monismith. (1996b) Development and Evaluation of Dynamic Flexural Beam Fatigue Test System. Transportation Research Record, no. 1545, Transportation Research Board, Washington, DC, pp. 89-97.

Tseng, K. H. and R. L. Lytton. (1990) Fatigue Damage Properties of Asphaltic Concrete Pavements. Transportation Research Record, no. 1286, Transportation Research Board, Washington, DC, pp. 84-97.

Van Dijk, W. (1975) Practical Fatigue Characterization of Bituminous Mixes. Proceedings of the Association of Asphalt Paving Technologists, vol. 44, pp. 38-74.

Van Dijk, W. and W. Visser. (1977) The Energy Approach to Fatigue for Pavement Design. Proceedings of the Association of Asphalt Paving Technologists, vol. 46, pp. 1-40.

VDOT. (1997) Metric Road and Bridge Specification. Virginia Department of Transportation, Richmond.

VDOT. (1999) Special Provisions for Section 211G Asphalt Concrete Mixtures. Virginia Department of Transportation, Richmond.

Von Quintus, H. L., J. B. Rauhut, and T. W. Kennedy. (1982) Comparisons of Asphalt Concrete Stiffness as Measured by Various Testing Techniques. Journal of the Association of Asphalt Paving Technologists, vol. 51, pp. 35-52.

APPENDIX A

Mixture Gradations

Figure A-1. Gradation of SM-9.5A, section D, F/F and F/L.

Sieve opening (mm)	Sieve #	% Passing	Control Point LL	Control Point UL	Restricted Zone LL	Restricted Zone UL	Result
12.5	1/2	99.3	-	100			F
9.5	3/8	92.4	90	100			P
4.75	#4	54.9	-	90			P
2.36	#8	34.8	32	67	47.2	47.2	P
1.18	#16	25.7	-	-	31.6	37.6	P
0.6	#30	20.4	-	-	23.5	27.5	P
0.3	#50	15.3	-	-	18.7	18.7	P
0.15	#100	11.8	-	-			
0.075	#200	9.2	2	10			P

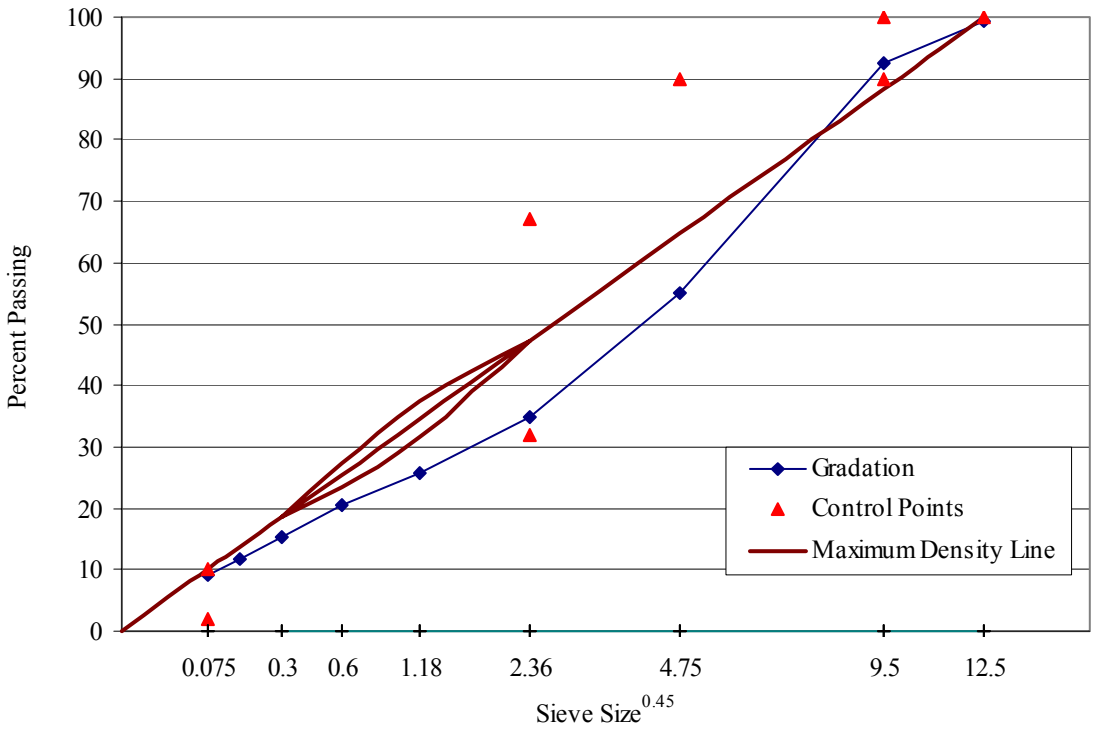

Figure A-2. Gradation of SM-9.5A, section D, L/L.

Sieve opening (mm)	Sieve #	% Passing	Control Point LL	Control Point UL	Restricted Zone LL	Restricted Zone UL	Result
12.5	1/2	100.0	-	100			F
9.5	3/8	89.3	90	100			P
4.75	#4	50.8	-	90			P
2.36	#8	37.0	32	67	47.2	47.2	P
1.18	#16	27.7	-	-	31.6	37.6	P
0.6	#30	20.4	-	-	23.5	27.5	P
0.3	#50	12.3	-	-	18.7	18.7	P
0.15	#100	8.0	-	-			
0.075	#200	5.7	2	10			P

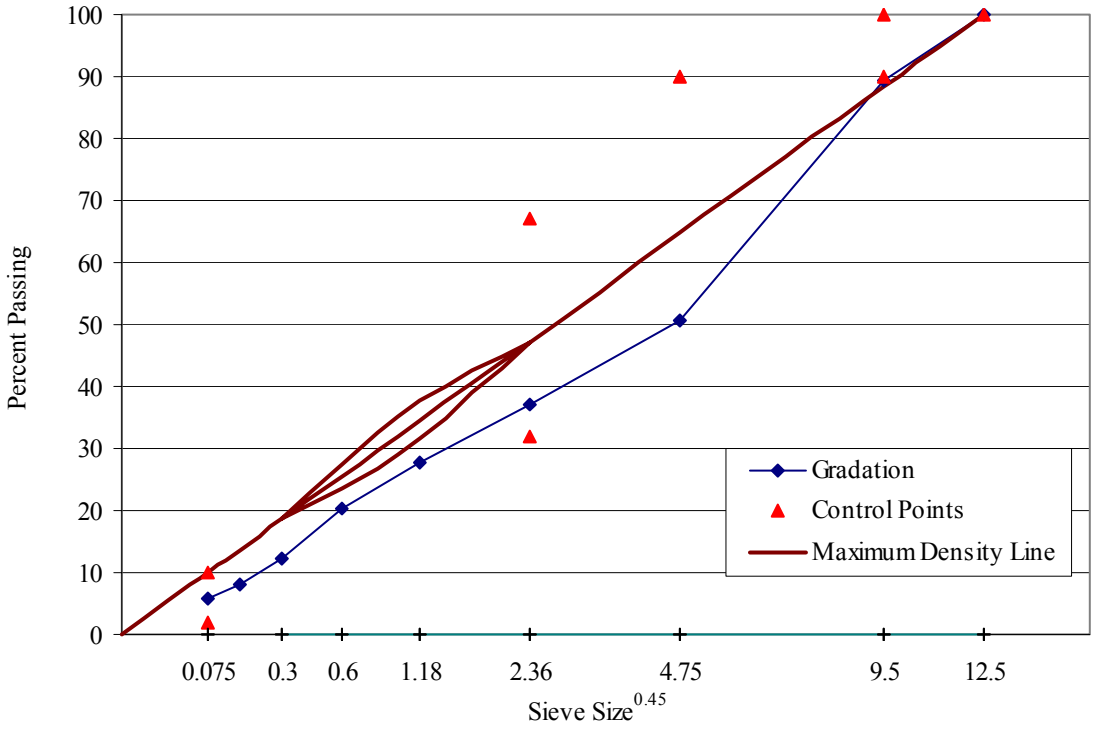

Figure A-3. Gradation of SM-9.5A, section D, D/L.

Sieve opening (mm)	Sieve #	% Passing	Control Point LL	Control Point UL	Restricted Zone LL	Restricted Zone UL	Result
12.5	1/2	99.2	-	100			F
9.5	3/8	92.3	90	100			P
4.75	#4	58.3	-	90			P
2.36	#8	41.7	32	67	47.2	47.2	P
1.18	#16	28.7	-	-	31.6	37.6	P
0.6	#30	20.3	-	-	23.5	27.5	P
0.3	#50	12.4	-	-	18.7	18.7	P
0.15	#100	8.6	-	-			
0.075	#200	6.3	2	10			P

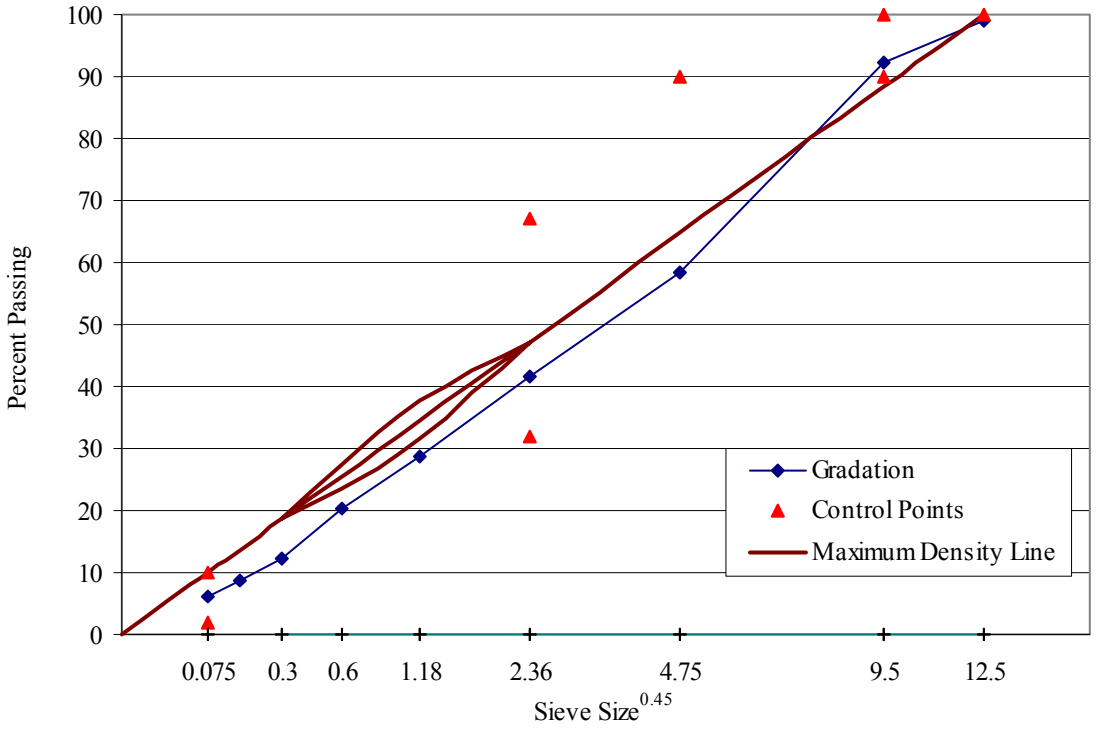

Figure A-4 Gradation of SM-9.5A, section I, F/F and F/L.

Sieve opening (mm)	Sieve #	% Passing	Control Point LL	Control Point UL	Restricted Zone LL	Restricted Zone UL	Result
12.5	1/2	100.0	-	100			P
9.5	3/8	95.0	90	100			P
4.75	#4	51.8	-	90			P
2.36	#8	35.0	32	67	47.2	47.2	P
1.18	#16	27.8	-	-	31.6	37.6	P
0.6	#30	20.6	-	-	23.5	27.5	P
0.3	#50	13.9	-	-	18.7	18.7	P
0.15	#100	10.6	-	-			
0.075	#200	7.3	2	10			P

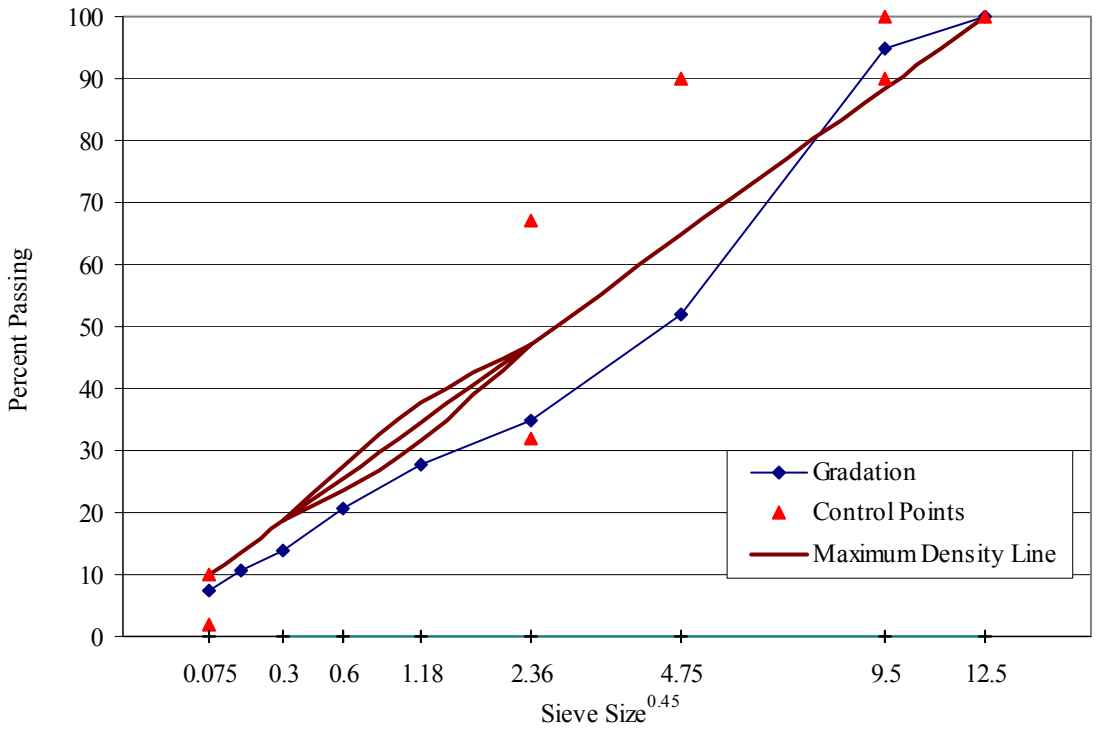

Figure A-5. Gradation of SM-9.5A, section I, L/L.

Sieve opening (mm)	Sieve #	% Passing	Control Point LL	Control Point UL	Restricted Zone LL	Restricted Zone UL	Result
12.5	1/2	99.4	-	100			F
9.5	3/8	92.7	90	100			P
4.75	#4	54.2	-	90			P
2.36	#8	37.6	32	67	47.2	47.2	P
1.18	#16	28.4	-	-	31.6	37.6	P
0.6	#30	21.2	-	-	23.5	27.5	P
0.3	#50	13.6	-	-	18.7	18.7	P
0.15	#100	9.6	-	-			
0.075	#200	7.0	2	10			P

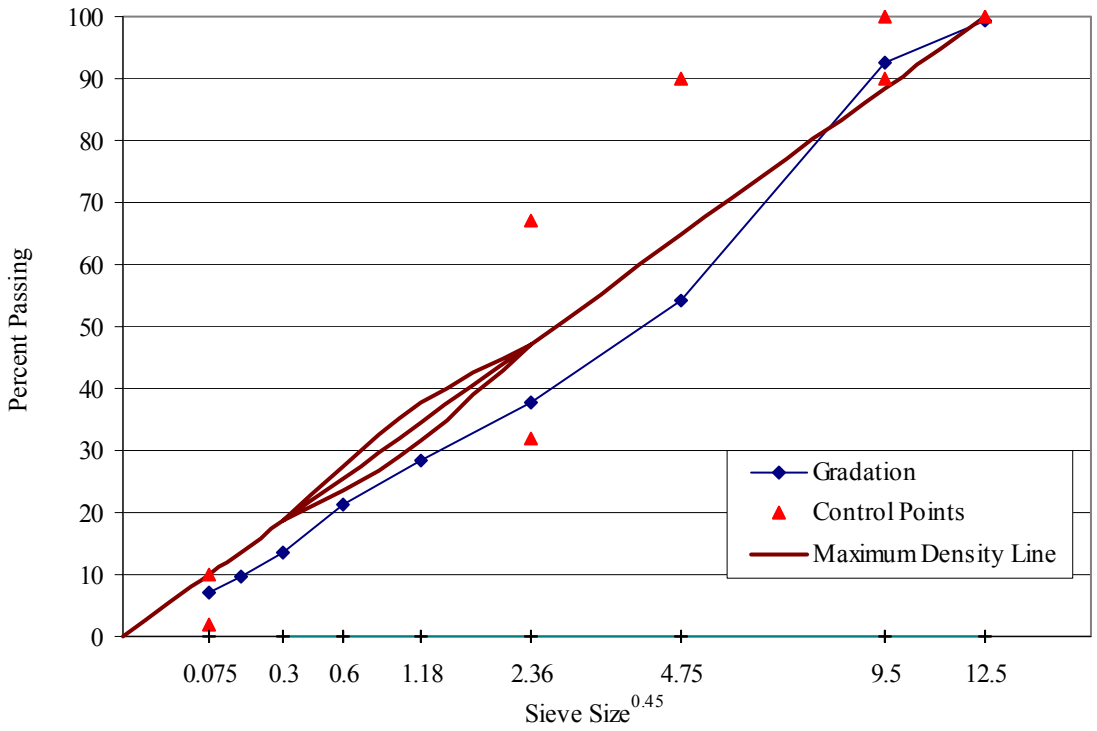

Figure A-6. Gradation of SM-9.5A, section I, D/L.

Sieve opening (mm)	Sieve #	% Passing	Control Point LL	Control Point UL	Restricted Zone LL	Restricted Zone UL	Result
12.5	1/2	98.9	-	100			F
9.5	3/8	88.6	90	100			P
4.75	#4	56.7	-	90			P
2.36	#8	43.5	32	67	47.2	47.2	P
1.18	#16	31.0	-	-	31.6	37.6	P
0.6	#30	22.1	-	-	23.5	27.5	P
0.3	#50	13.9	-	-	18.7	18.7	P
0.15	#100	10.1	-	-			
0.075	#200	7.6	2	10			P

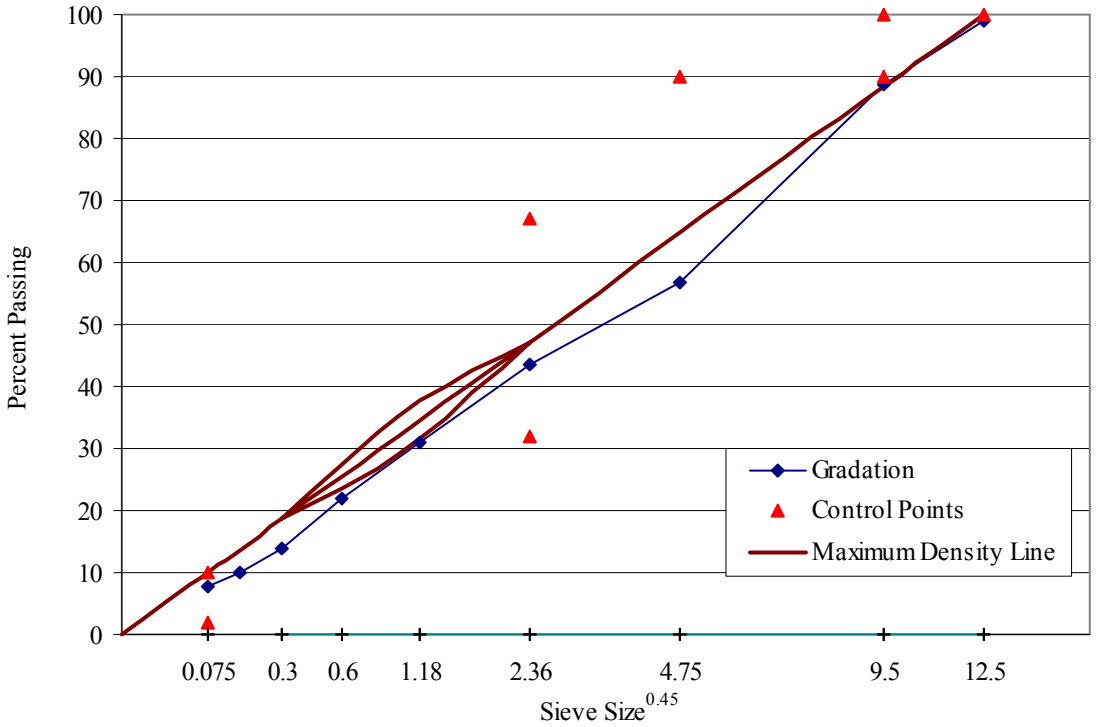

Figure A-7. Gradation of SM-9.5D, section B, F/F and F/L.

Sieve opening (mm)	Sieve #	% Passing	Control Point LL	Control Point UL	Restricted Zone LL	Restricted Zone UL	Result
12.5	1/2	98.5	-	100			F
9.5	3/8	90.3	90	100			P
4.75	#4	51.9	-	90			P
2.36	#8	35.4	32	67	47.2	47.2	P
1.18	#16	26.7	-	-	31.6	37.6	P
0.6	#30	18.1	-	-	23.5	27.5	P
0.3	#50	11.9	-	-	18.7	18.7	P
0.15	#100	9.4	-	-			
0.075	#200	7.8	2	10			P

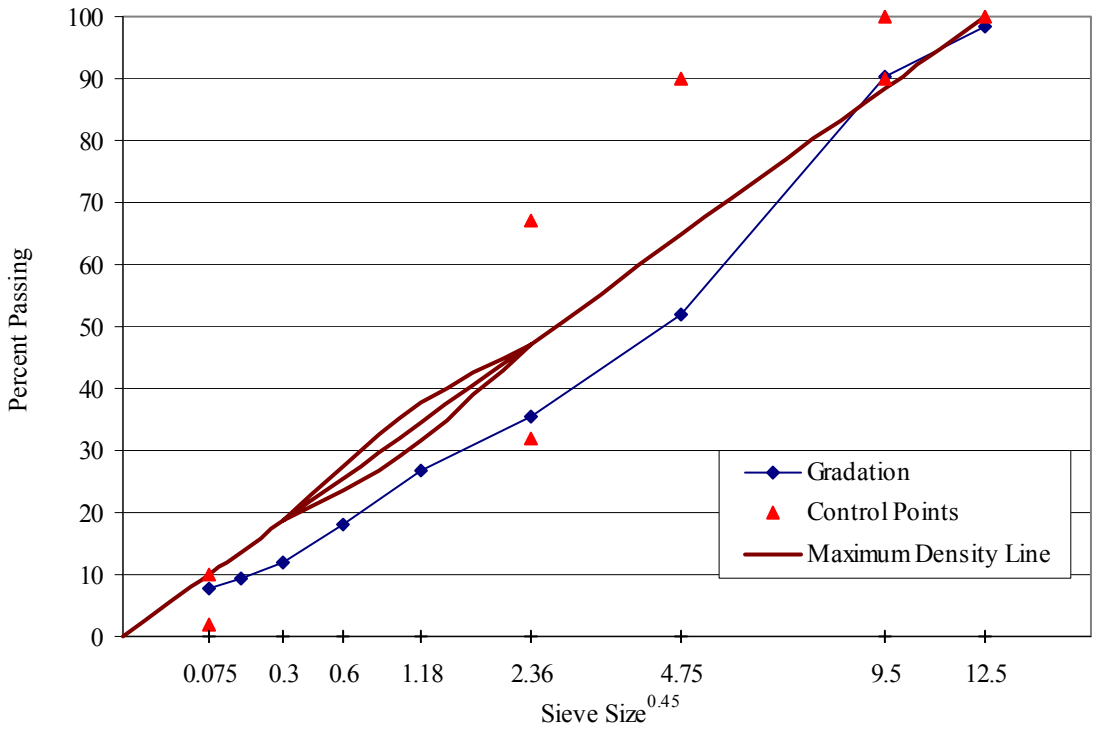

Figure A-8. Gradation of SM-9.5D, section B, L/L.

Sieve opening (mm)	Sieve #	% Passing	Control Point LL	Control Point UL	Restricted Zone LL	Restricted Zone UL	Result
12.5	1/2	98.5	-	100			F
9.5	3/8	91.5	90	100			P
4.75	#4	58.8	-	90			P
2.36	#8	42.5	32	67	47.2	47.2	P
1.18	#16	30.8	-	-	31.6	37.6	P
0.6	#30	22.9	-	-	23.5	27.5	P
0.3	#50	15.1	-	-	18.7	18.7	P
0.15	#100	11.1	-	-			
0.075	#200	8.7	2	10			P

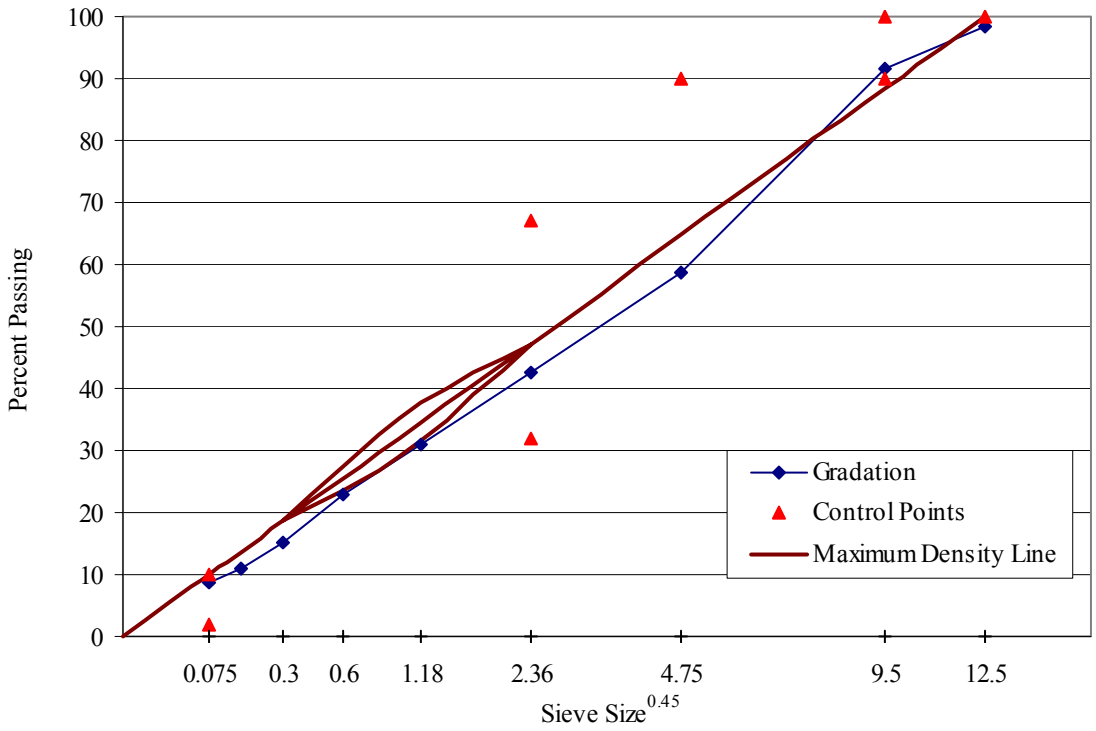

Figure A-9. Gradation of SM-9.5D, section B, D/L.

Sieve opening (mm)	Sieve #	% Passing	Control Point LL	Control Point UL	Restricted Zone LL	Restricted Zone UL	Result
12.5	1/2	99.7	-	100			F
9.5	3/8	86.1	90	100			P
4.75	#4	33.7	-	90			P
2.36	#8	22.9	32	67	47.2	47.2	F
1.18	#16	18.2	-	-	31.6	37.6	P
0.6	#30	14.0	-	-	23.5	27.5	P
0.3	#50	8.8	-	-	18.7	18.7	P
0.15	#100	6.6	-	-			
0.075	#200	5.5	2	10			P

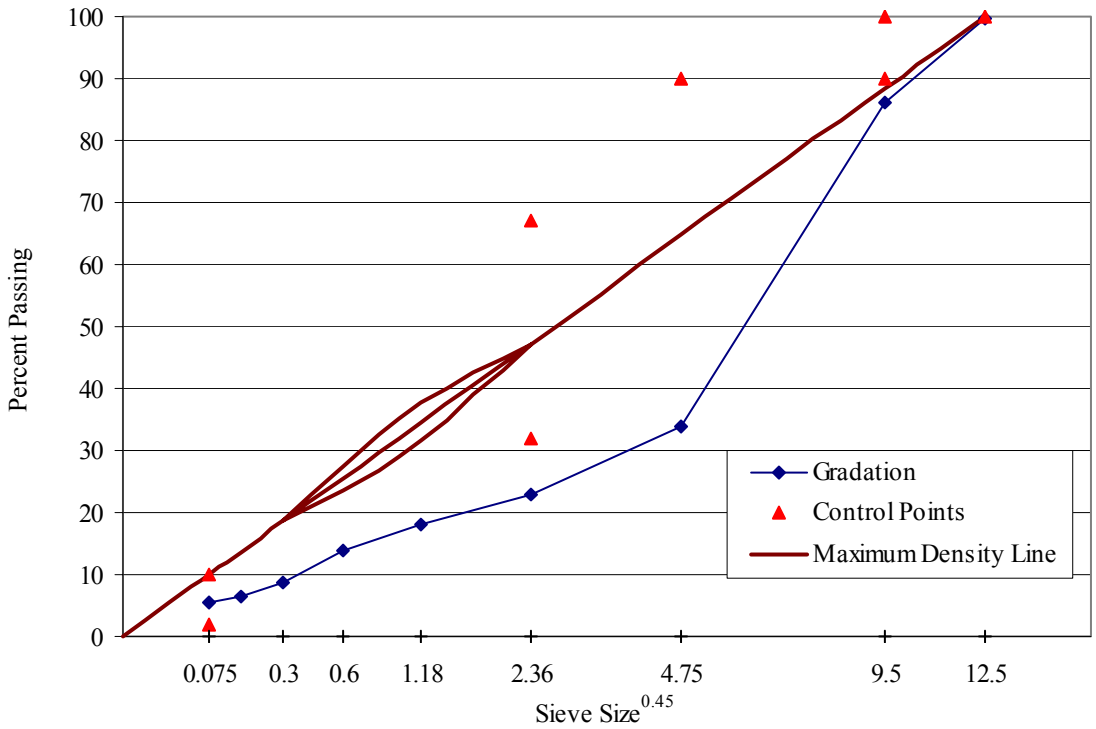

Figure A-10. Gradation of SM-9.5D, section E, F/F and F/L.

Sieve opening (mm)	Sieve #	% Passing	Control Point LL	Control Point UL	Restricted Zone LL	Restricted Zone UL	Result
12.5	1/2	97.6	-	100			F
9.5	3/8	92.9	90	100			P
4.75	#4	63.3	-	90			P
2.36	#8	42.6	32	67	47.2	47.2	P
1.18	#16	31.5	-	-	31.6	37.6	P
0.6	#30	20.5	-	-	23.5	27.5	P
0.3	#50	13.3	-	-	18.7	18.7	P
0.15	#100	10.4	-	-			
0.075	#200	7.6	2	10			P

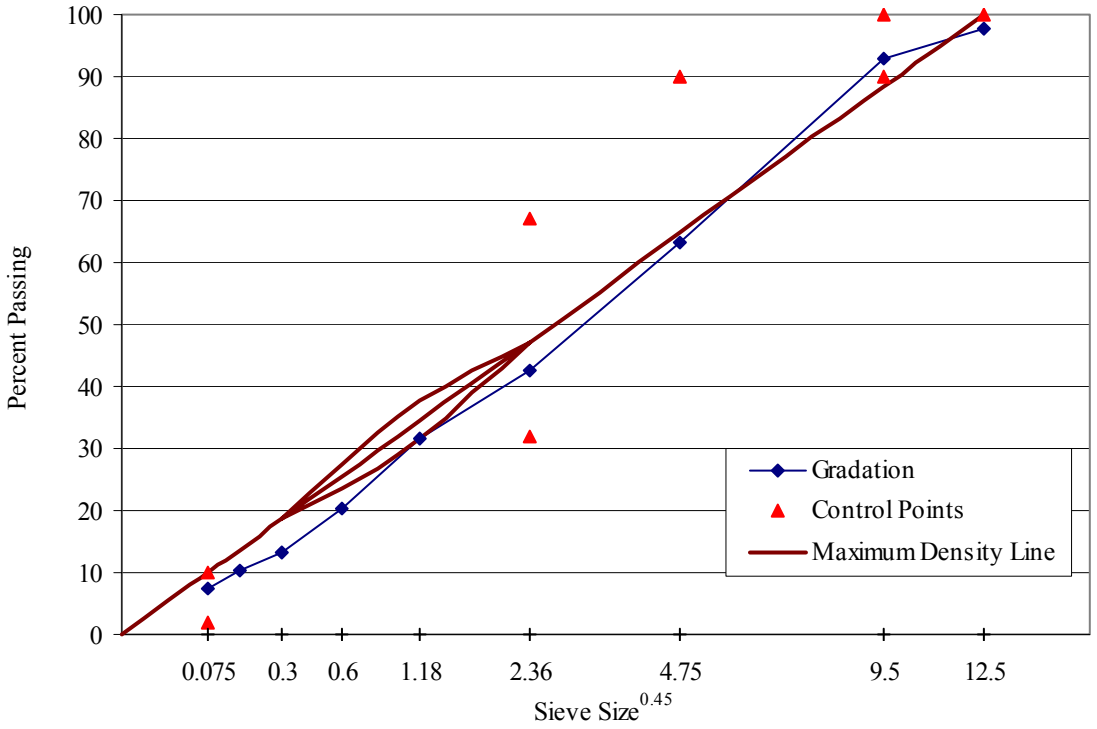

Figure A-11. Gradation of SM-9.5D, sections E, F, G, and H, L/L.

Sieve opening (mm)	Sieve #	% Passing	Control Point LL	Control Point UL	Restricted Zone LL	Restricted Zone UL	Result
12.5	1/2	99.3	-	100			F
9.5	3/8	93.0	90	100			P
4.75	#4	61.4	-	90			P
2.36	#8	42.4	32	67	47.2	47.2	P
1.18	#16	31.0	-	-	31.6	37.6	P
0.6	#30	23.0	-	-	23.5	27.5	P
0.3	#50	15.2	-	-	18.7	18.7	P
0.15	#100	11.1	-	-			
0.075	#200	8.5	2	10			P

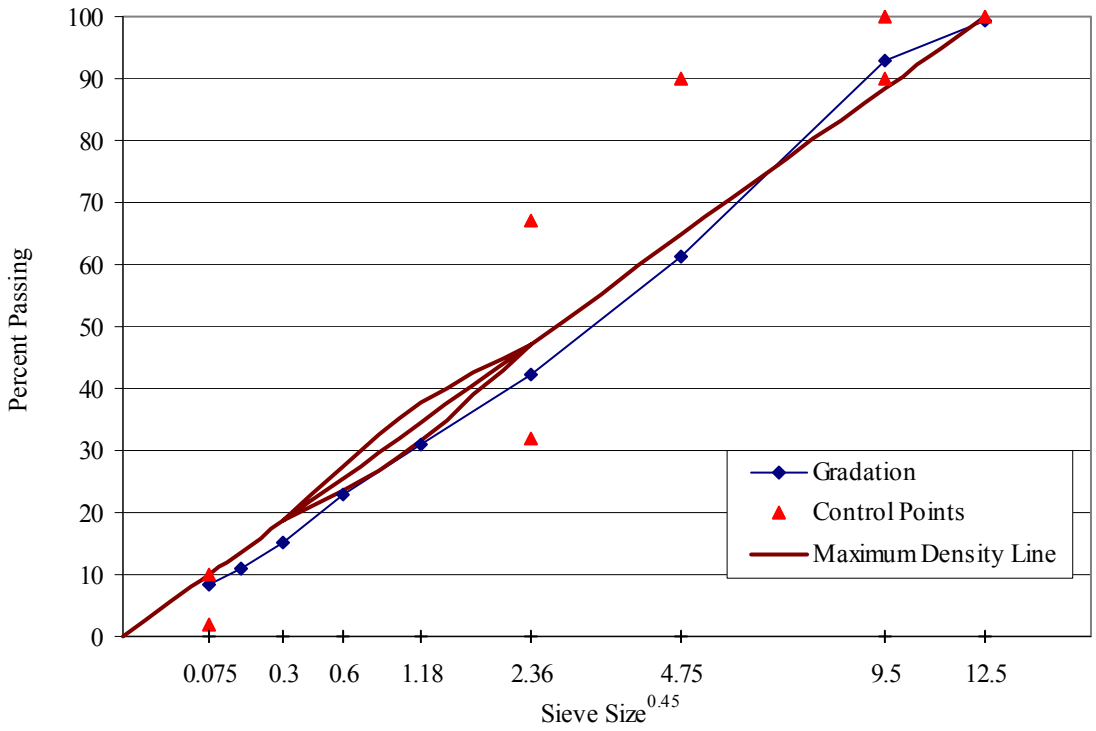

Figure A-12. Gradation of SM-9.5D, section F, F/F and F/L.

Sieve opening (mm)	Sieve #	% Passing	Control Point LL	Control Point UL	Restricted Zone LL	Restricted Zone UL	Result
12.5	1/2	99.4	-	100			F
9.5	3/8	93.4	90	100			P
4.75	#4	56.7	-	90			P
2.36	#8	38.6	32	67	47.2	47.2	P
1.18	#16	25.7	-	-	31.6	37.6	P
0.6	#30	18.4	-	-	23.5	27.5	P
0.3	#50	12.1	-	-	18.7	18.7	P
0.15	#100	8.7	-	-			
0.075	#200	6.9	2	10			P

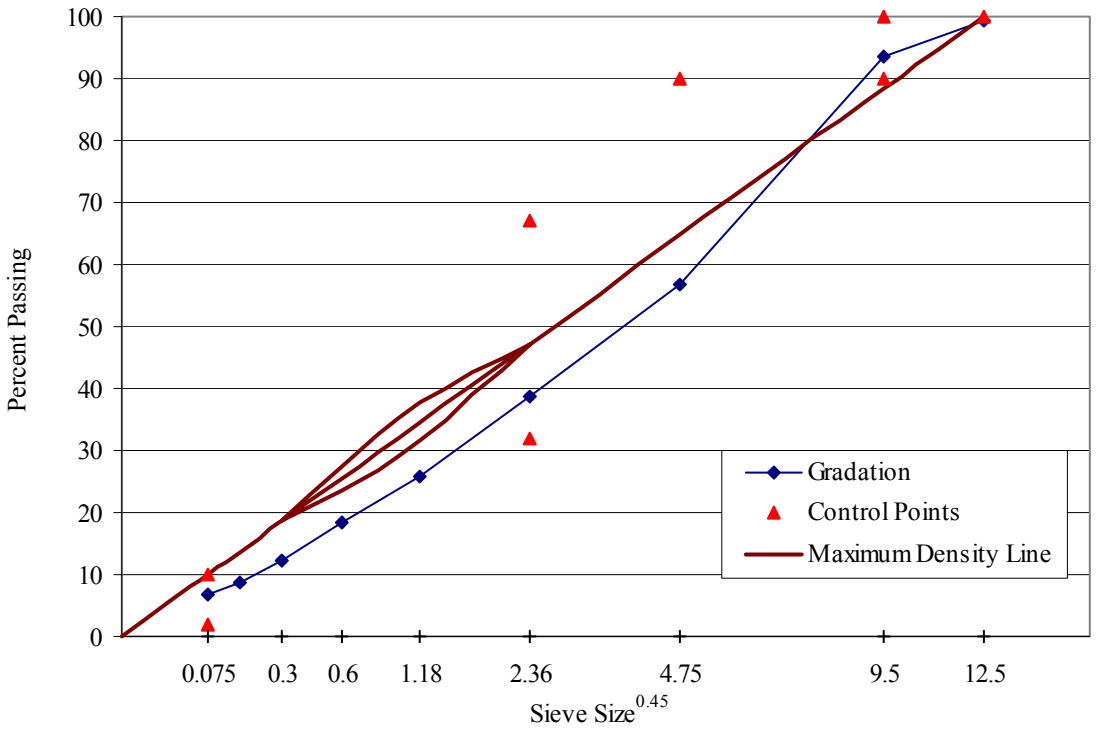

Figure A-13. Gradation of SM-9.5D, section G, F/F and F/L.

Sieve opening (mm)	Sieve #	% Passing	Control Point LL	Control Point UL	Restricted Zone LL	Restricted Zone UL	Result
12.5	1/2	98.4	-	100			F
9.5	3/8	95.1	90	100			P
4.75	#4	62.3	-	90			P
2.36	#8	42.2	32	67	47.2	47.2	P
1.18	#16	28.9	-	-	31.6	37.6	P
0.6	#30	20.9	-	-	23.5	27.5	P
0.3	#50	13.8	-	-	18.7	18.7	P
0.15	#100	10.3	-	-			
0.075	#200	8.3	2	10			P

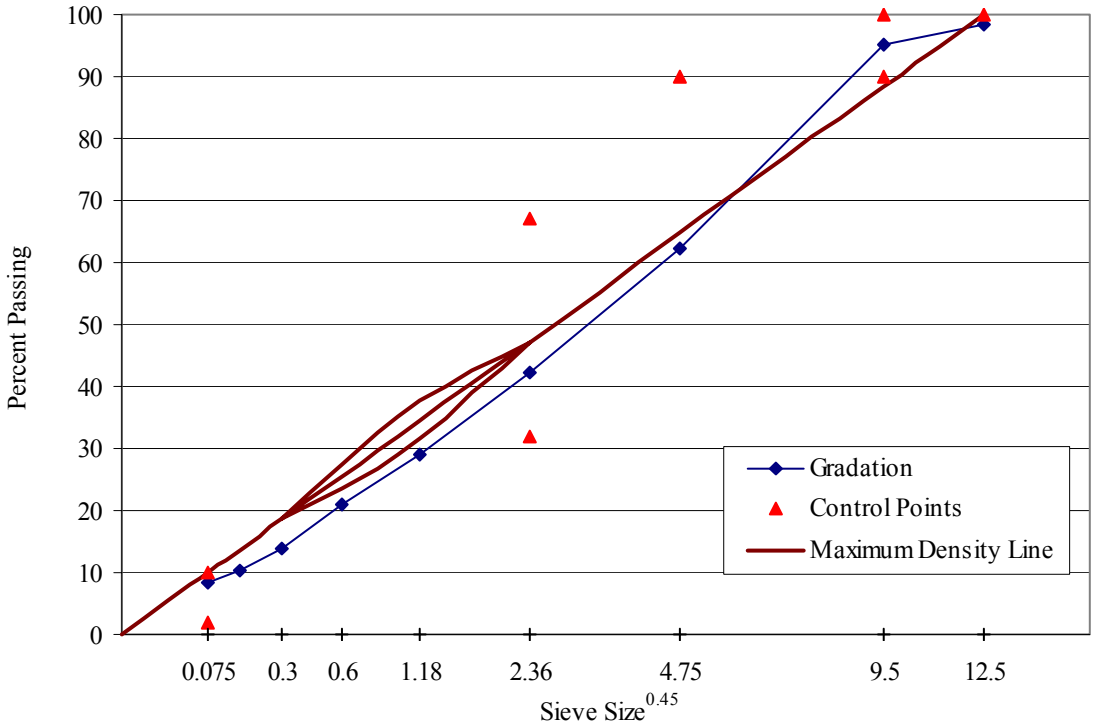

Figure A-14. Gradation of SM-9.5D, section H, F/F and F/L.

Sieve opening (mm)	Sieve #	% Passing	Control Point LL	Control Point UL	Restricted Zone LL	Restricted Zone UL	Result
12.5	1/2	98.3	-	100			F
9.5	3/8	94.3	90	100			P
4.75	#4	63.8	-	90			P
2.36	#8	43.1	32	67	47.2	47.2	P
1.18	#16	29.3	-	-	31.6	37.6	P
0.6	#30	20.9	-	-	23.5	27.5	P
0.3	#50	13.5	-	-	18.7	18.7	P
0.15	#100	9.6	-	-			
0.075	#200	7.6	2	10			P

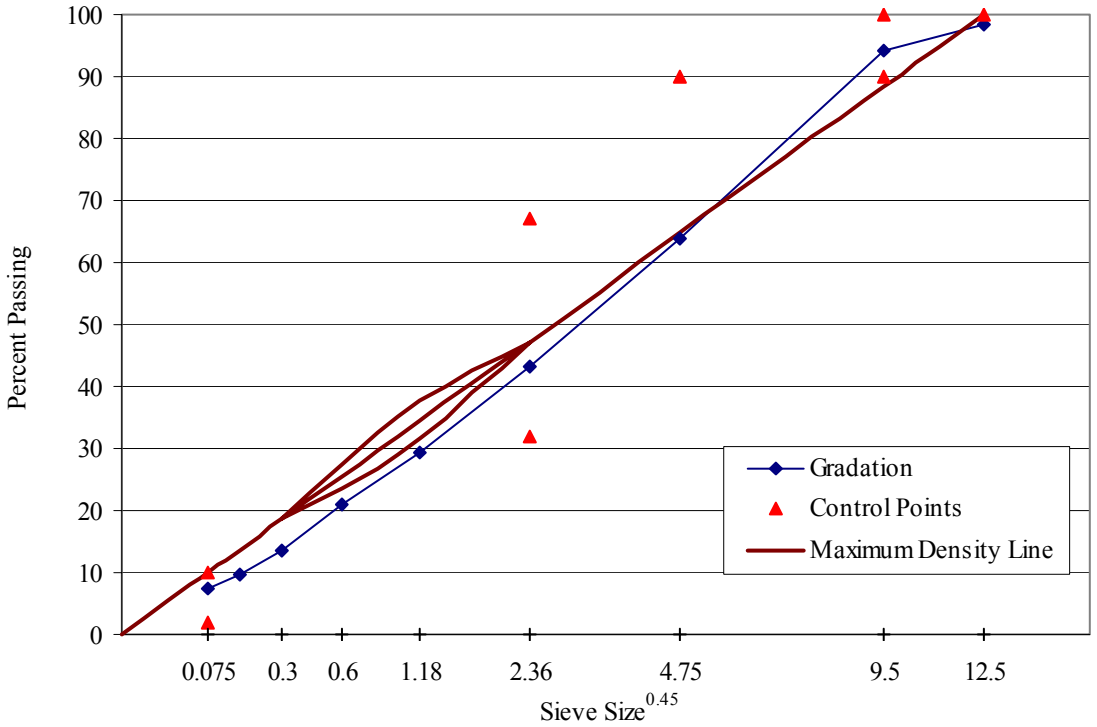

Figure A-15. Gradation of SM-9.5D, section J, F/F and F/L.

Sieve opening (mm)	Sieve #	% Passing	Control Point LL	Control Point UL	Restricted Zone LL	Restricted Zone UL	Result
12.5	1/2	99.2	-	100			F
9.5	3/8	91.6	90	100			P
4.75	#4	50.5	-	-			
2.36	#8	34.6	32	67	47.2	47.2	P
1.18	#16	26.2	-	-	31.6	37.6	P
0.6	#30	17.9	-	-	23.5	27.5	P
0.3	#50	11.8	-	-	18.7	18.7	P
0.15	#100	9.1	-	-			
0.075	#200	6.3	2	10			P

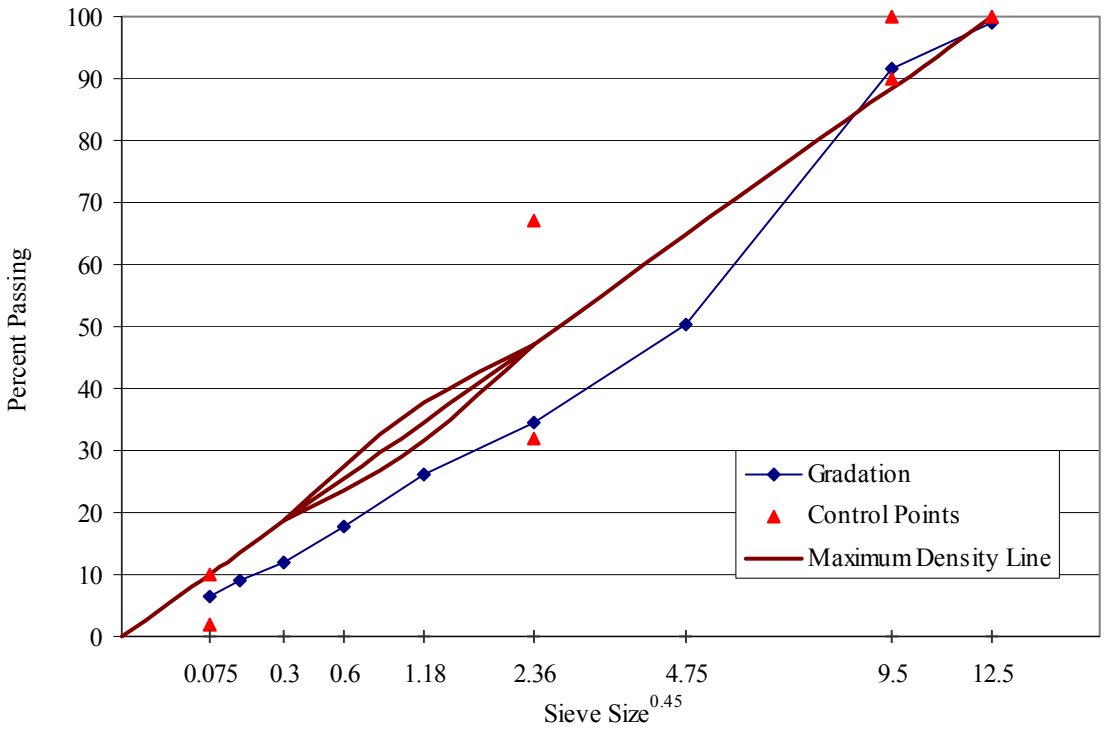

Figure A-16. Gradation of SM-9.5D, section J, L/L.

Sieve opening (mm)	Sieve #	% Passing	Control Point LL	Control Point UL	Restricted Zone LL	Restricted Zone UL	Result
12.5	1/2	100.0	-	100			P
9.5	3/8	93.9	90	100			P
4.75	#4	52.9	-	-			
2.36	#8	31.6	32	67	47.2	47.2	F
1.18	#16	22.8	-	-	31.6	37.6	P
0.6	#30	17.4	-	-	23.5	27.5	P
0.3	#50	11.2	-	-	18.7	18.7	P
0.15	#100	8.4	-	-			
0.075	#200	6.7	2	10			P

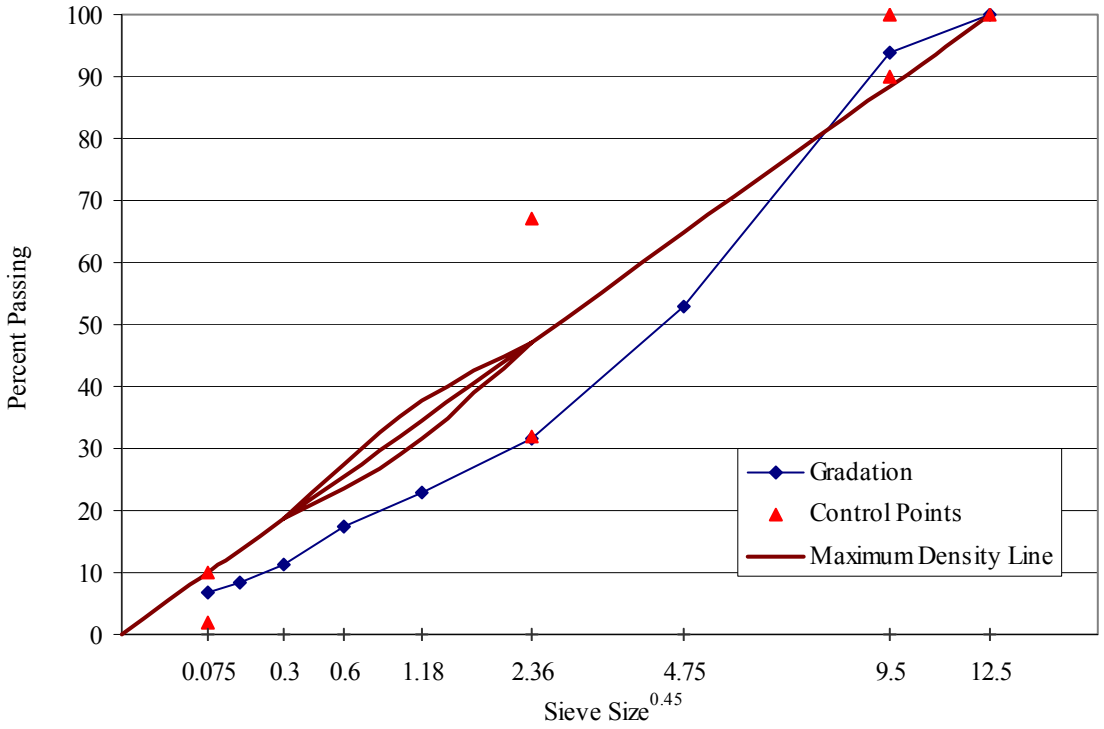

Figure A-17. Gradation of SM-9.5E, section C, F/F and F/L.

Sieve opening (mm)	Sieve #	% Passing	Control Point LL	Control Point UL	Restricted Zone LL	Restricted Zone UL	Result
12.5	1/2	98.0	-	100			F
9.5	3/8	90.9	90	100			P
4.75	#4	55.3	-	90			P
2.36	#8	34.3	32	67	47.2	47.2	P
1.18	#16	27.0	-	-	31.6	37.6	P
0.6	#30	19.7	-	-	23.5	27.5	P
0.3	#50	14.1	-	-	18.7	18.7	P
0.15	#100	11.1	-	-			
0.075	#200	8.0	2	10			P

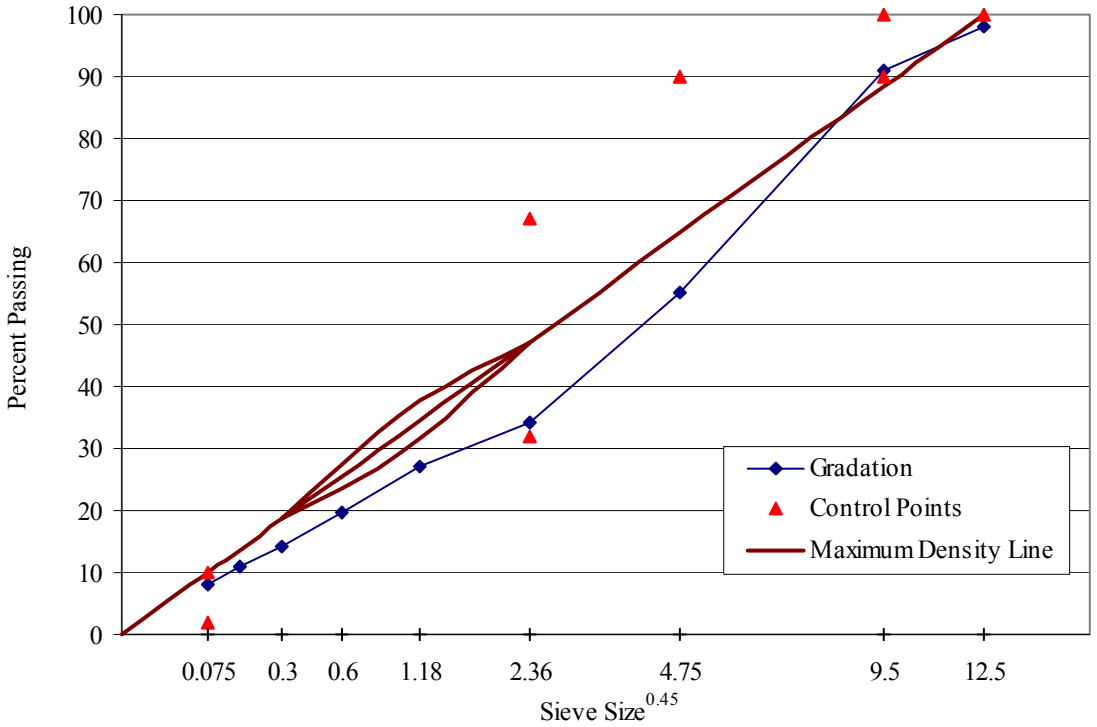

Figure A-18. Gradation of SM-9.5E, section C, L/L.

Sieve opening (mm)	Sieve #	% Passing	Control Point LL	Control Point UL	Restricted Zone LL	Restricted Zone UL	Result
12.5	1/2	99.7	-	100			F
9.5	3/8	90.2	90	100			P
4.75	#4	44.6	-	90			P
2.36	#8	35.2	32	67	47.2	47.2	P
1.18	#16	27.3	-	-	31.6	37.6	P
0.6	#30	21.0	-	-	23.5	27.5	P
0.3	#50	13.8	-	-	18.7	18.7	P
0.15	#100	10.1	-	-			
0.075	#200	7.6	2	10			P

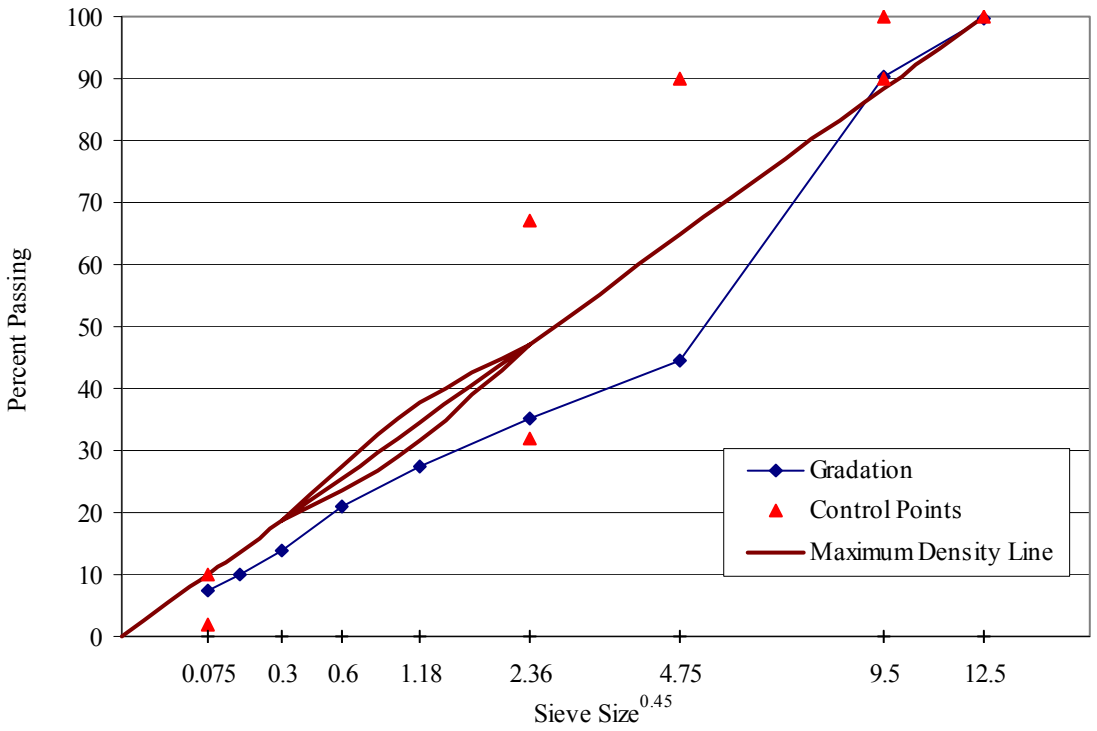

Figure A-19. Gradation of SM-9.5E,, section C, D/L.

Sieve opening (mm)	Sieve #	% Passing	Control Point LL	Control Point UL	Restricted Zone LL	Restricted Zone UL	Result
12.5	1/2	99.4	-	100			F
9.5	3/8	86.5	90	100			F
4.75	#4	44.9	-	90			P
2.36	#8	32.8	32	67	47.2	47.2	P
1.18	#16	25.2	-	-	31.6	37.6	P
0.6	#30	19.3	-	-	23.5	27.5	P
0.3	#50	12.5	-	-	18.7	18.7	P
0.15	#100	8.9	-	-			
0.075	#200	6.6	2	10			P

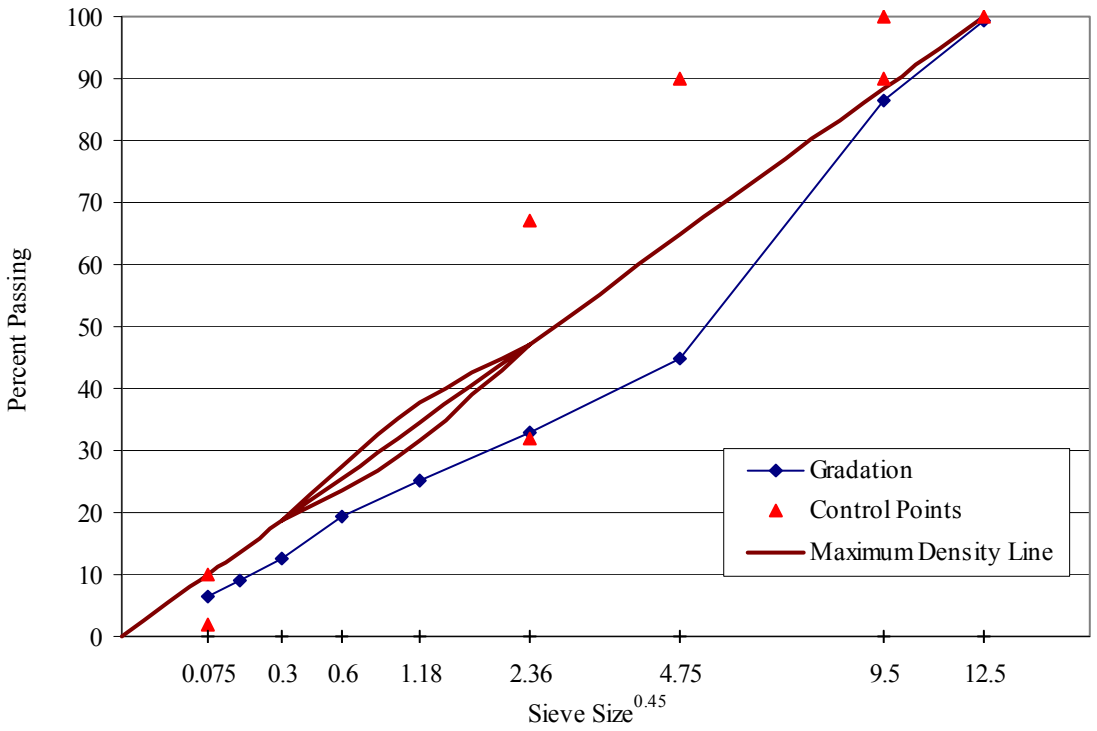

Figure A-20. Gradation of SM-12.5D, section A, F/F and F/L.

Sieve opening (mm)	Sieve #	% Passing	Control Point LL	Control Point UL	Restricted Zone LL	Restricted Zone UL	Result
19	3/4	100.0		100			P
12.5	1/2	99.6	90	100			P
9.5	3/8	98.5	-	90			F
4.75	#4	84.2	-	-			
2.36	#8	47.7	28	58	39.1	39.1	P
1.18	#16	37.3	-	-	25.6	31.6	P
0.6	#30	27.0	-	-	19.1	23.1	P
0.3	#50	14.7	-	-	15.5	15.5	P
0.15	#100	10.2	-	-			
0.075	#200	5.6	2	10			P

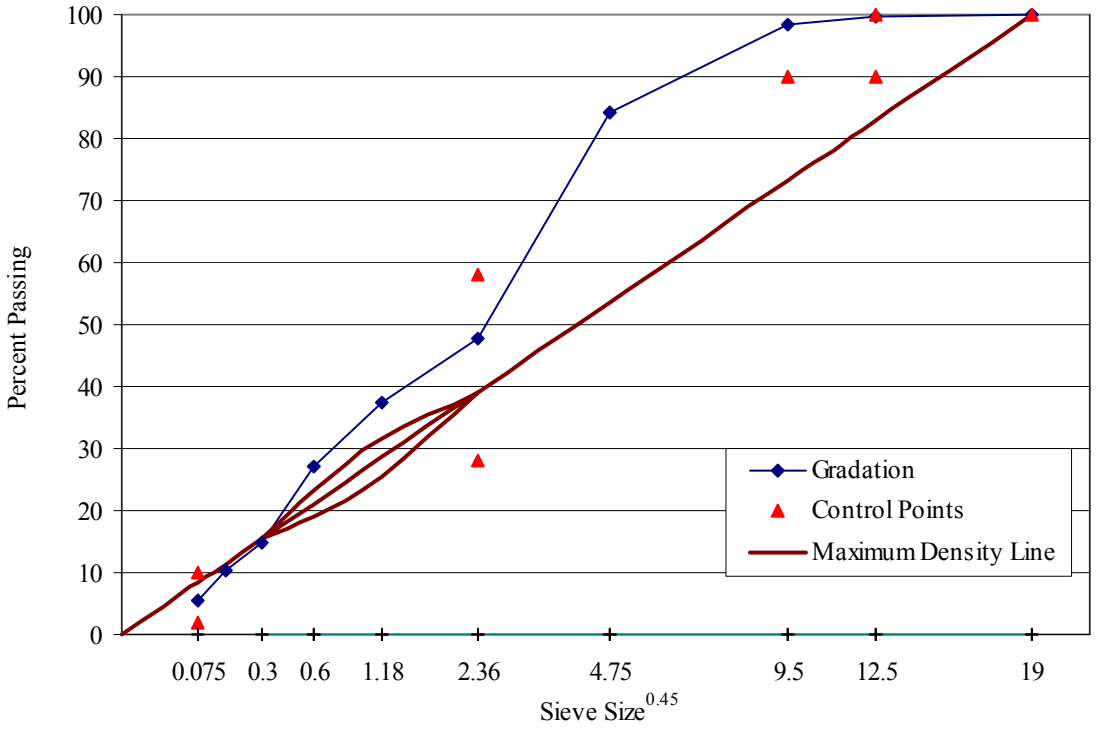

Figure A-21. Gradation of SM-12.5D, section A, L/L.

Sieve opening (mm)	Sieve #	% Passing	Control Point LL	Control Point UL	Restricted Zone LL	Restricted Zone UL	Result
19	3/4	100.0		100			P
12.5	1/2	99.5	90	100			P
9.5	3/8	98.9	-	90			F
4.75	#4	91.3	-	-			
2.36	#8	58.3	28	58	39.1	39.1	F
1.18	#16	38.8	-	-	25.6	31.6	P
0.6	#30	28.7	-	-	19.1	23.1	P
0.3	#50	20.1	-	-	15.5	15.5	P
0.15	#100	15.6	-	-			
0.075	#200	12.3	2	10			F

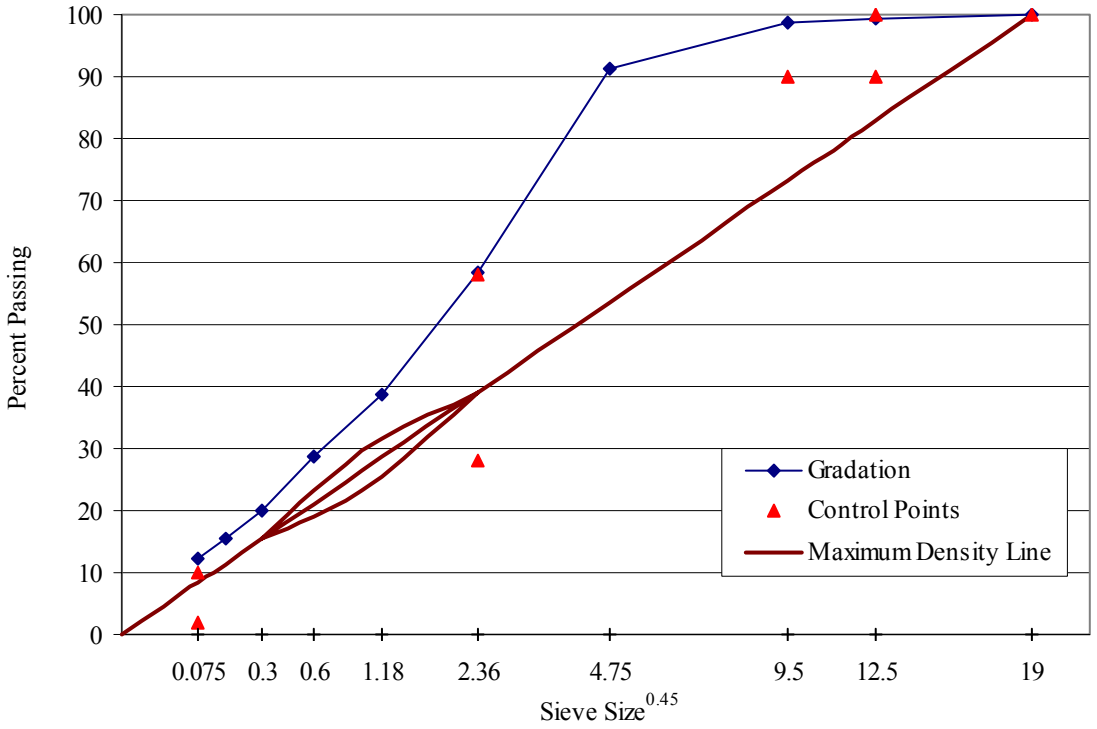

Figure A-22. Gradation of SM-12.5D, section A, D/L

Sieve #	% Passing	Control Point LL	Control Point UL	Restricted Zone LL	Restricted Zone UL	Result
3/4	100.0		100			P
1/2	98.4	90	100			P
3/8	89.9	-	90			P
#4	50.1	-	-			
#8	27.7	28	58	39.1	39.1	F
#16	20.2	-	-	25.6	31.6	P
#30	15.3	-	-	19.1	23.1	P
#50	9.7	-	-	15.5	15.5	P
#100	7.3	-	-			
#200	6.0	2	10			P

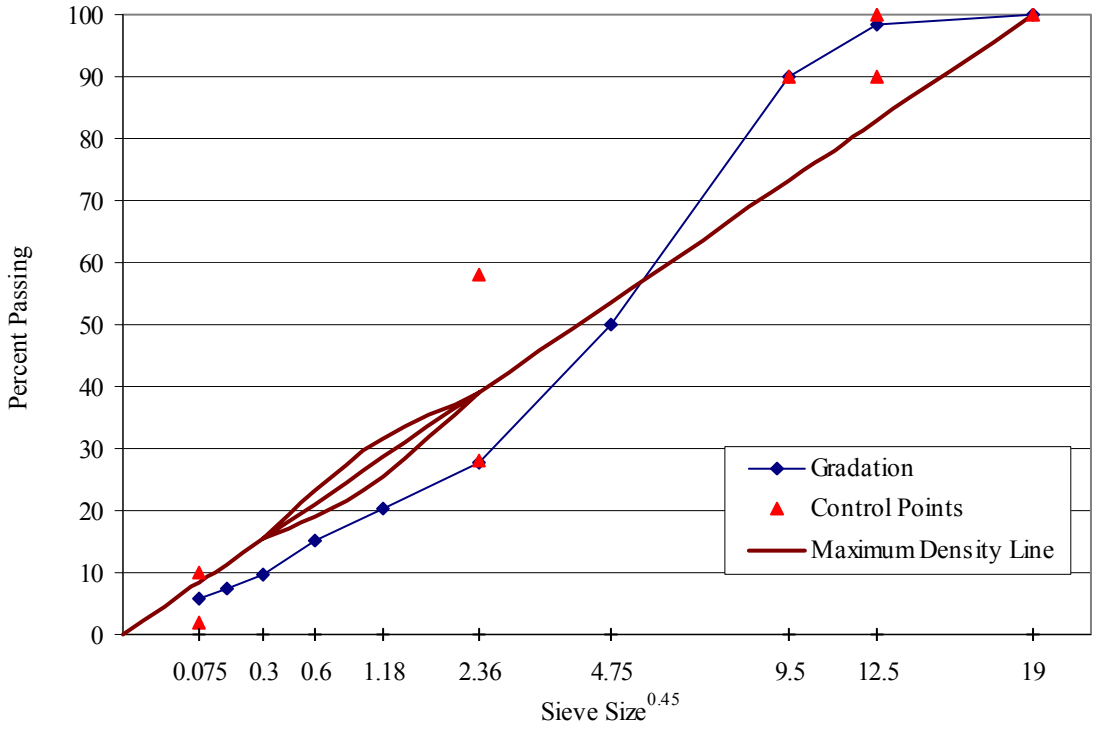

Figure A-23. Gradation of SMA-12.5, section L, F/F and F/L.

Sieve opening (mm)	Sieve #	% Passing	Control Point LL	Control Point UL	Restricted Zone LL	Restricted Zone UL	Result
19	3/4	100.0		100			
12.5	1/2	99.4	90	100			P
9.5	3/8	87.7	-	90			P
4.75	#4	36.8	-	-			
2.36	#8	25.0	28	58	39.1	39.1	F
1.18	#16	21.4	-	-	25.6	31.6	P
0.6	#30	18.9	-	-	19.1	23.1	P
0.3	#50	16.1	-	-	15.5	15.5	P
0.15	#100	13.9	-	-			
0.075	#200	11.2	2	10			F

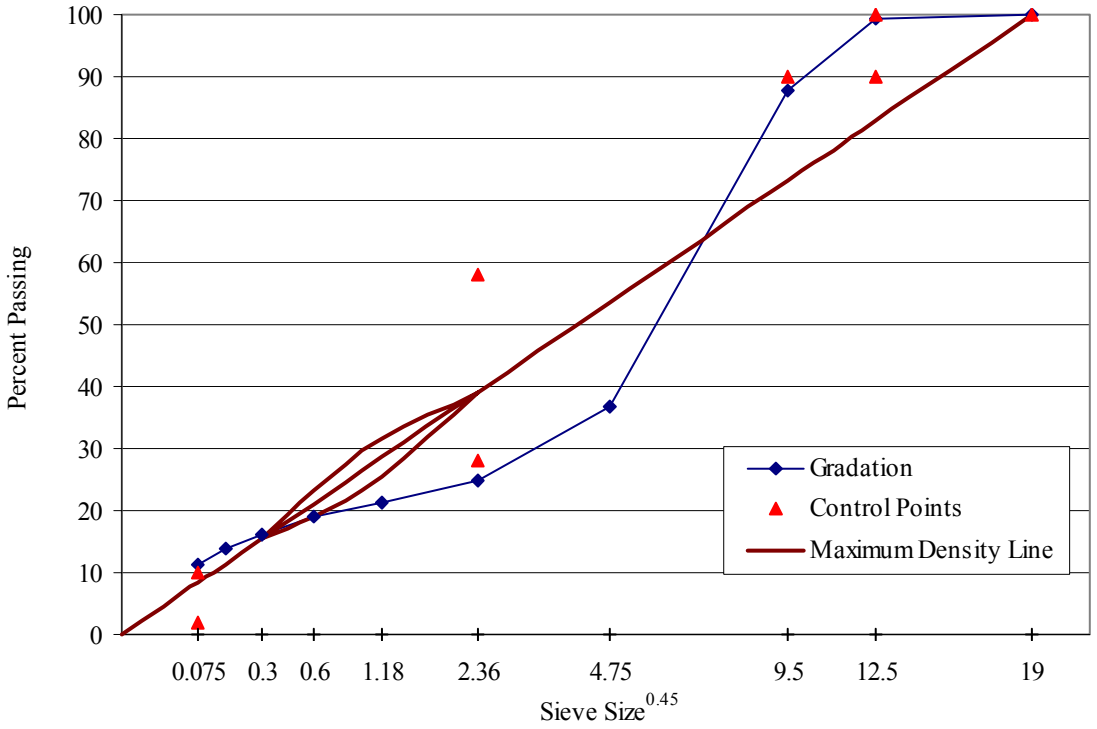

Figure A-24. Gradation of SMA-12.5, section L, L/L.

Sieve opening (mm)	Sieve #	% Passing	Control Point LL	Control Point UL	Restricted Zone LL	Restricted Zone UL	Result
19	3/4	100.0		100			
12.5	1/2	92.8	90	100			P
9.5	3/8	76.3	-	90			P
4.75	#4	28.1	-	-			
2.36	#8	21.8	28	58	39.1	39.1	F
1.18	#16	17.9	-	-	25.6	31.6	P
0.6	#30	15.3	-	-	19.1	23.1	P
0.3	#50	14.0	-	-	15.5	15.5	P
0.15	#100	13.1	-	-			
0.075	#200	11.7	2	10			F

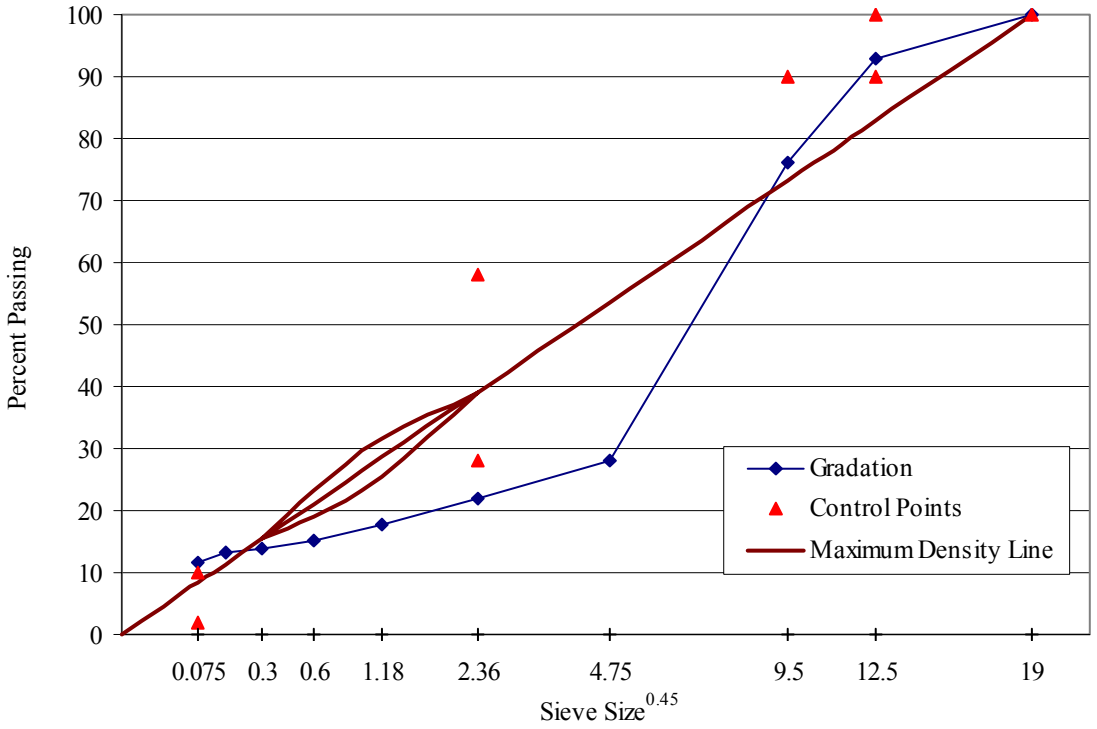

Figure A-25. Gradation of SMA-12.5, section L, D/L.

Sieve opening (mm)	Sieve #	% Passing	Control Point LL	Control Point UL	Restricted Zone LL	Restricted Zone UL	Result
19	3/4	100.0		100			
12.5	1/2	92.6	90	100			P
9.5	3/8	72.1	-	90			P
4.75	#4	27.8	-	-			
2.36	#8	19.5	28	58	39.1	39.1	F
1.18	#16	16.7	-	-	25.6	31.6	P
0.6	#30	14.8	-	-	19.1	23.1	P
0.3	#50	13.7	-	-	15.5	15.5	P
0.15	#100	12.9	-	-			
0.075	#200	11.7	2	10			F